COPY 1

DOT/FAA/CT-81/69-I

Dayton Aircraft Cabin Fire Model, Version 3, Volume I - Physical Description

FEDERAL AVIATION ADMINISTRATION

JUL 12 1982

TECHNICAL CENTER LIBRARY
ATLANTIC CITY, N.J. 08405

Charles D. MacArthur
University of Dayton Research Institute
Dayton, Ohio 45469

June 1982

Final Report

This document is available to the U.S. public through the National Technical Information Service, Springfield, Virginia 22161.

U.S. Department of Transportation
Federal Aviation Administration
Technical Center
Atlantic City Airport, N.J. 08405

Technical Report Documentation Page

1. Report No.	2. Government Accession No.	3. Recipient's Catalog No.
DOT/FAA/CT-81/69-I		

4. Title and Subtitle	5. Report Date
Dayton Aircraft Cabin Fire Model Version 3 Volume 1 - Physical Description	June 1982
	6. Performing Organization Code
	8. Performing Organization Report No.
7. Author(s) Charles D. MacArthur	UDRI-TR-81-159
9. Performing Organization Name and Address University of Dayton Research Institute 300 College Park Avenue Dayton, Ohio 45469	10. Work Unit No. (TRAIS)
	11. Contract or Grant No. DOT-FA74WA-3532
	13. Type of Report and Period Covered Final Report 01 April 1980-31 March 1981
12. Sponsoring Agency Name and Address U.S. Department of Transportation Federal Aviation Administration FAA Technical Center Atlantic City, New Jersey 08405	14. Sponsoring Agency Code

15. Supplementary Notes

16. Abstract

Version 3 of the Dayton Aircraft Cabin Fire Model (DACFIR) has been created as a refinement and generalization of earlier mathematical models for the computer simulation of fire growth in the cabin of a commercial transport airplane. The model uses data from laboratory tests on the cabin furnishing materials and a zone (control volume) representation of the cabin atmosphere to predict the accumulation of heat, smoke, and gases resulting from arbitrary ignition sources specified in the program input. The major improvements included in Version 3 are a revised cabin atmosphere model which allows for multiple compartments and the prescribed entry of exterior fire gases, and an implicit numerical integration technique for the atmosphere equations. Volume I of this report contains a full description of the model's predictions to the results of three full-scale cabin fire tests. Volume II consists of appendices which include a user's guide and listing of the computer code.

17. Key Words	18. Distribution Statement
aircraft fire safety, fire research, aircraft interior materials, smoke and toxic gases, aircraft cabin fires, enclosed fire, fire tests, mathematical fire model, computer simulation	Document is available to the public through the National Technical Information Service Springfield, Virginia 22151

19. Security Classif. (of this report)	20. Security Classif. (of this page)	21. No. of Pages	22. Price
UNCLASSIFIED	UNCLASSIFIED	52	

Form DOT F 1700.7 (8-72) Reproduction of completed page authorized

PREFACE

This report was prepared by the University of Dayton Research Institute for the Federal Aviation Administration Technical Center under Contract FA74WA-3532 during the period April 1980 through March 1981. The report describes the third refined version of the Dayton Aircraft Cabin Fire Model (DACFIR).

Work was performed at the University of Dayton under the supervision of Nicholas Engler. Others at the University who contributed to this program are John Myers, Steven Vondrell, Thomas Shirley, and Zalfa Challita. Much of the original development of the DACFIR model is due to Jerry Reeves, Peter Kahut, and James Luers. The author wishes to thank Gretchen Walther, Jacquelin Aldrich, Nahla Abdelnour, and Pamela Ecker for their assistance in preparing this report.

TABLE OF CONTENTS

LIST OF ILLUSTRATIONS

LIST OF TABLES

SECTION 1
INTRODUCTION

1.1 PURPOSE

The report describes Version 3 of the Dayton Aircraft Cabin Fire Model (DACFIR3), a mathematical model of fire within the cabin of a commercial transport aircraft. DACFIR3 is the most recent refinement of models developed to predict the accumulation of smoke, heat, and toxic gases in a cabin by using laboratory test data on the cabin interior materials. The refined model takes into account compartmentation of the cabin and the entry of the flames and gases of an external fire. In addition, DACFIR3 incorporates a number of recent advances in theory and practice of modeling enclosed fires.

1.2 BACKGROUND

The DACFIR model was developed to better understand the relationship of small-scale fire test data on individual cabin materials to the behavior of these materials when involved in an actual full-scale fire. For many reasons, this relationship is not always straightforward. This fact has obvious bearing on fire safety standards for cabin materials. Mathematical modeling and computer simulation of cabin fire development provides one means of clarifying the relationship by making it possible to account for the complex geometry of the cabin and the various conditions of ignition, fire exposure, and ventilation.

The first version of DACFIR, described in Reference 1, predicted fire spread and smoke, heat, and gas accumulation for complex cabin geometries but was limited to wide-body cabin configurations. In order to compare the prediction of the model to existing fire test data on standard width cabins, a number of refinements and extensions were made (Reference 2) which resulted in the second version, DACFIR2. This second version accomodates both standard and wide-body cabins and predicts oxygen concentration in the cabin atmosphere in addition to the original quantities. Other refinements included adding a capability for forced ventilation in improvements to the methods of computing flame and gas radiation.

Recent test and experiment work (References 3, 4, 5, and 6) has focused attention upon a highly probable mode of ignition for cabin fires--the entry of flames, radiation, and gases of an exterior fire through a cabin door or other opening. The first two versions of the model addressed only fires originating within the cabin, and so cannot be used to study this interesting case. Also, division or compartmentation of the cabin to contain a growing fire has been proposed as a fire safety measure. This concept has been examined experimentally (Reference 7) but no theoretical methods for its study have been available. Finally, a number of advances (e.g., References 8 and 9) in both the theory and practice of modeling enclosed fires have appeared since the original conception of DACFIR that can be incorporated in the model to bring it up to current standards.

These three factors--interest in exterior fire ignition, in compartmentation, and the current improvements in mathematical fire modeling--

have resulted in a third version of DACFIR which is the subject of this report. The report is divided into two volumes. The first volume presents the assumptions, theory, and formulation of DACFIR3 including a brief description of the computer code. Volume 2 contains several appendices on derivations of some of the model equations, a user's guide for the DACFIR3 program, and a listing of the computer code.

SECTION 2

STRUCTURE OF THE MODEL

The formulation, assumptions, and structure of the DACFIR model reflect the model's basic purpose: to predict the accumulation of smoke, heat, and toxic gases during the emergency evacuation period. Our interest is in the conditions which may impede evacuation and the role the cabin materials have in the development of these conditions. Therefore the model deals with the early stages of the fire; that is, times when only a small percentage of all the cabin materials are involved. During this period the cabin is filling with combustion products but evacuation may still be possible. The rate at which the cabin becomes uninhabitable is the key factor that the model seeks to predict. This time scale--perhaps the first five or ten minutes after a fire develops in the cabin--has the major influence on the model's structure in terms of the physical processes that must be considered and how the processes are handled mathematically.

Because the model must attempt to deal comprehensively with all the important phenomena of the problem, the level of detail and sophistication of the component pieces of the model is necessarily somewhat simple. However, when the simple models of each phenomenon are assembled into the complete system, the resulting structure is complex. This section gives an overview of the complete model by briefly explaining the modeling techniques and assumption and the relationship among them. More detailed explanations of the separate components are given in Sections 3, 4, and 5.

2.1 CABIN GEOMETRY AND FIRE GROWTH

The DACFIR model considers fires originating on and propagating over the fixed interior surface of the cabin. The model makes detailed predictions of the areas of each type of material on fire at any time. The rate at which a fire develops depends upon the types of materials, the orientation of the burning surface, and the thermal conditions in the cabin. We approximate the cabin geometry as being constructed of only horizontal or vertical surfaces. This assumption simplifies the calculations for simulating the fire growth while retaining the important geometric features. The method of predicting the burning area on each surface uses a gridding scheme which divides the fuel surface into discrete regions. Each surface within the cabin is divided into equal size squares using a grid of vertical and horizontal lines. A convenient dimension for the square size is six inches (0.5 ft) on a side. These fuel squares are referred to as "elements" in the model. Figure 1 illustrates how the cabin interior is approximated in this method. Seciton 3 presents the details of the gridding scheme.

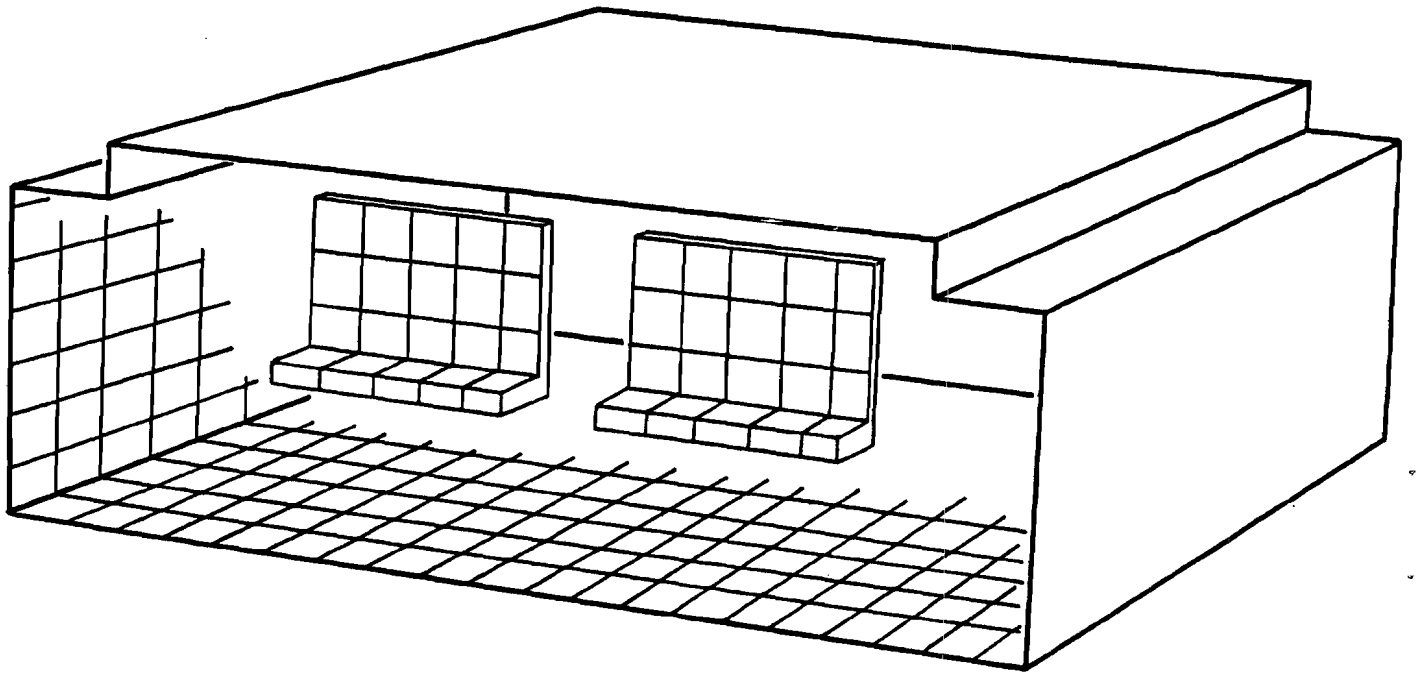

Figure 1. DACFIR Representation of Cabin Interior.

The total material surface on fire is determined by keeping track of which elements are burning at any given time. A single fire (or, more correctly, fire base area) is defined as a number of contiguous burning elements. Other elements might be smoldering (undergoing non-flaming pryrolysis) while still others may be as yet unaffected by the fire, or be burned-out or "charred." The spread of the fires is simulated by igniting at appropriate times elements adjacent to burning elements or by igniting elements touched by the flames of a fire originating on some other surface. The problem of tracking the development of a fire then becomes one of determining when and if elements change from a non-burning to a burning condition and from burning to burned-out. These transitions are taken to be functions of the current fire situation and the flammability characteristics of the materials comprising the various surfaces.

The flammability characteristics of the materials--flame spread rates; ignition delay times; heat, smoke, and gas release rates; etc.--are rarely well defined and certainly not as well understood as the more convential thermodynamic and mechanical properties. The present state of knowledge about the

combustion of solids does not let us obtain the pertinent flammability characteristics from first principles for the complex materials and structures of an aircraft cabin. However, these characteristics may be measured directly in laboratory experiments. The DACFIR model has been developed assuming that these characteristics can be supplied as input data. The specific material flammability information used by DACFIR is shown in Table 1.

These flammability characteristics are not intrinsic material properties but are also functions of exterior conditions during burning. For DACFIR we have made the simplifying assumption that these items are functions only of the externally applied radiation flux. While this is certainly an oversimplification, since other factors such as fraction burned or sample orientation are definitely important, current opinion (e.g. Reference 10) holds that flame radiation has the dominant effect on burning rate for fires of the scale considered by DACFIR3.

Table 1 contains two emission rates for each material, one for smoldering and the other for burning (open flaming). The smoldering condition is initiated when the heat flux to the element reaches a specified level and the material decomposes without flames. Smoke and toxic gases are emitted at a constant rate until (1) the heat flux is reduced below the specified level, (2) the element changes to the burning state by the propagation of the fire, or (3) the element is charred. Once the material begins flaming combustion, it is assumed to emit smoke, toxic gases, and heat until the material is charred. Thus the model assumes that the flaming state is self-sustaining while the smoldering state requires a minimum level of exterior heating to continue.

2.2 MODELING THE CABIN ATMOSPHERE

DACFIR3 uses the "zone" method of modeling the accumulation of combustion products in the cabin atmospheres. Zone models have been used by a number of investigators for analyzing fires in residential buildings in the past few years and this method is developing into somewhat of a standard technique (reference 11). The method has proven to be a practical first approximation for the complex problem of the fluid dynamics and heat transfer of fire in room-sized enclosures.

The basic assumption of zone modeling is that the hot combustion products rising from the flames gather at the compartment ceiling to form a well-mixed zone or layer. As the fire progresses, more and more of the original uncontaminated gas in the lower region of the compartment is "pumped" through the flames and plume to enter the hot upper zone. As long as the compartment volume is not large, the turbulent mixing caused by the rapidly rising fire gases is sufficient to keep the upper products zone well-mixed, which results in a uniform temperature and composition. This model, generally supported by experimental observations, allows a simple, lumped parameter treatment of the conservation equations for the cabin atmosphere. Single values of temperature, density, and species mass fractions are used to describe the upper and lower zones. The boundary between the zones, the "thermal discontinuity," is assumed to be a horizontal plane parallel to the cabin floor. The volumes of the upper and lower zones are defined by the position of this plane and the

walls, ceiling, floor, and partitions of the compartment. Figure 2 shows the main features of the two-zone approximation. When the cabin is divided into several compartments, the two-zone approximation applies to each compartment--when, of course, conditions are such that some hot gases have penetrated into every compartment.

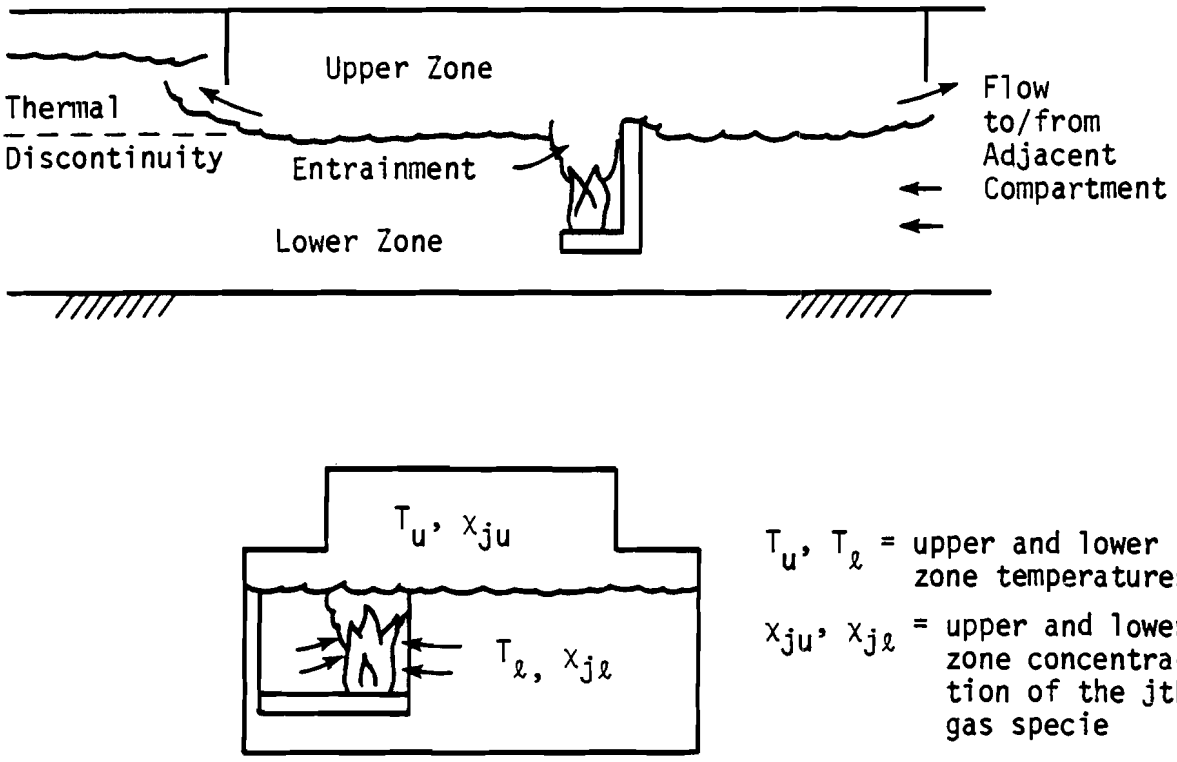

Figure 2. Zone Model of the Compartment Atmosphere.

The simulation of the behavior of the cabin atmosphere consists of numerically solving the conservation equations for each zone in one or more compartments for the values of temperature, smoke and species concentration, and other gas properties as simulated time progresses. Heat, smoke, and gas accumulation are of primary interst because of their effect on emergency evacuation. We are also interested in the thermal radiation from the hot upper zone to the burning or about-to-be-ignited materials. This radiation will supplement the local flame radiation to increase the flame spread and emission rates of the materials. In this way, the cabin atmosphere is coupled to the fire development processes. Details of the cabin atmosphere model are given in Section 4.

TABLE 1

MATERIAL FLAMMABILITY CHARACTERISTICS USED AS INPUT FOR DACFIR3

Symbol	Description
f_h	Horizontal flame spread rate.
f_u	Upward flame spread rate.
f_d	Downward flame spread rate.
t_f	Time interval from flame contact to the start of flaming combustion.
t_{fc}	Time interval from the start to the end of flaming combustion.
r_h	Heat release rate per unit area during flaming.
r_{sf}	Smoke release rate per unit during flaming.
$r_f(i)$	Release rate per unit area of the ith gas specie during flaming.
q_p	Heat flux at which the material begins to smolder.
t_p	Time interval from the time at which the exosure flux reaches q_p to the start of smoldering.
t_{pc}	Time interval from the start of smoldering to the consumption of the material.
t_{pe}	Time required for smoldering to stop after the heat flux falls below q_p.
r_{ss}	Smoke release rate per unit area during smoldering.
$r_s(i)$	Release rate of the ith gas specie during smoldering.
ΔH_c	Effective heat of combustion.
γ	Stoichiometric oxygen-to-fuel mass ratio
ρ_f	Pyrolyzate vapor density.
u_f	Pyrolyzate vapor surface blowing velocity.
R_f	Radiated fraction of ΔH_c

2.3 RADIATION MODELING

As explained above, the primary parameter determining the fire growth rate in DACFIR is the level of thermal radiation reaching the burning and smoldering materials. Calculation of the radiation intensities, however, is a difficult problem. While much work has been done on the radiation of medium-scale diffusion flames, the results are still limited to simple geometries, e.g., horizontal pool fires or vertical wall fires. Added to this is the fact that precise radiation calculations are inherently complicated and highly dependent on the exact flame geometry and temperature. For these reasons the DACFIR model must use simple, approximate relationships for flame radiation. The computations assume a cylindrical flame volume of uniform fixed temperature; spectrally gray emissivity; and a height proportional to the hydraulic radius of the base area. Further, for materials within the base reagion, no variation of flux with position is assumed; and an average value for all elements in the base is used. This method cannot be regarded as precise in any detail, but it provides an indication of the relative radiation intensity and therefore of the materials' behavior. This level of approximation is justified partly by the practical problems encountered when more detailed methods are used and partly by the degree to which the materials' properties are known as functions of radiation.

2.4 ORGANIZATION OF THE COMPUTATIONS

The DACFIR model is implemented as FORTRAN computer program which integrates the differential equations and simulates the fire spread for a given set of initial conditions. The solution of the differential equation set describing the cabin atmopshere requires an implicit integration method and a relatively small time step, on the order of one second or less. The simulation of fire growth, however, proceeds somewhat more slowly--for most cases, several seconds may pass between the ignition of new material elements. The program is designed to deal efficiently with these different time scales by using a nested loop structure as shown in Figure 3. During a run integration of the cabin atmosphere equations proceeds at a given time step, Δt. At a pre-set interval, usually five seconds, the program reviews the status of all burning and smoldering elements and makes the required ignitions, burn-outs, changes of emission rate, etc. This procedure can continue until all the cabin materials considered by the model have burned-up, but normally we are only interested in about the first ten minutes of the fire.

The other important point shown in Figure 3 is the loop structure for dealing wtih individual fires. Subroutine SCAN identifies connected groups of burning elements which form the base planes of fires. As each group is identified and isolated, the flame volume, local radiation levels, and the spread of burning caused by this group are found by the subroutines which follow SCAN. If there are additional burning elements, control returns to SCAN to build the additional fire bases and compute the spread caused by them. When all elements on all surfaces have been searched and the new growth computed, the new total rates of heat and mass emission are updated prior to entering the cabin atmosphere routines controlled by subroutine ATMOS.

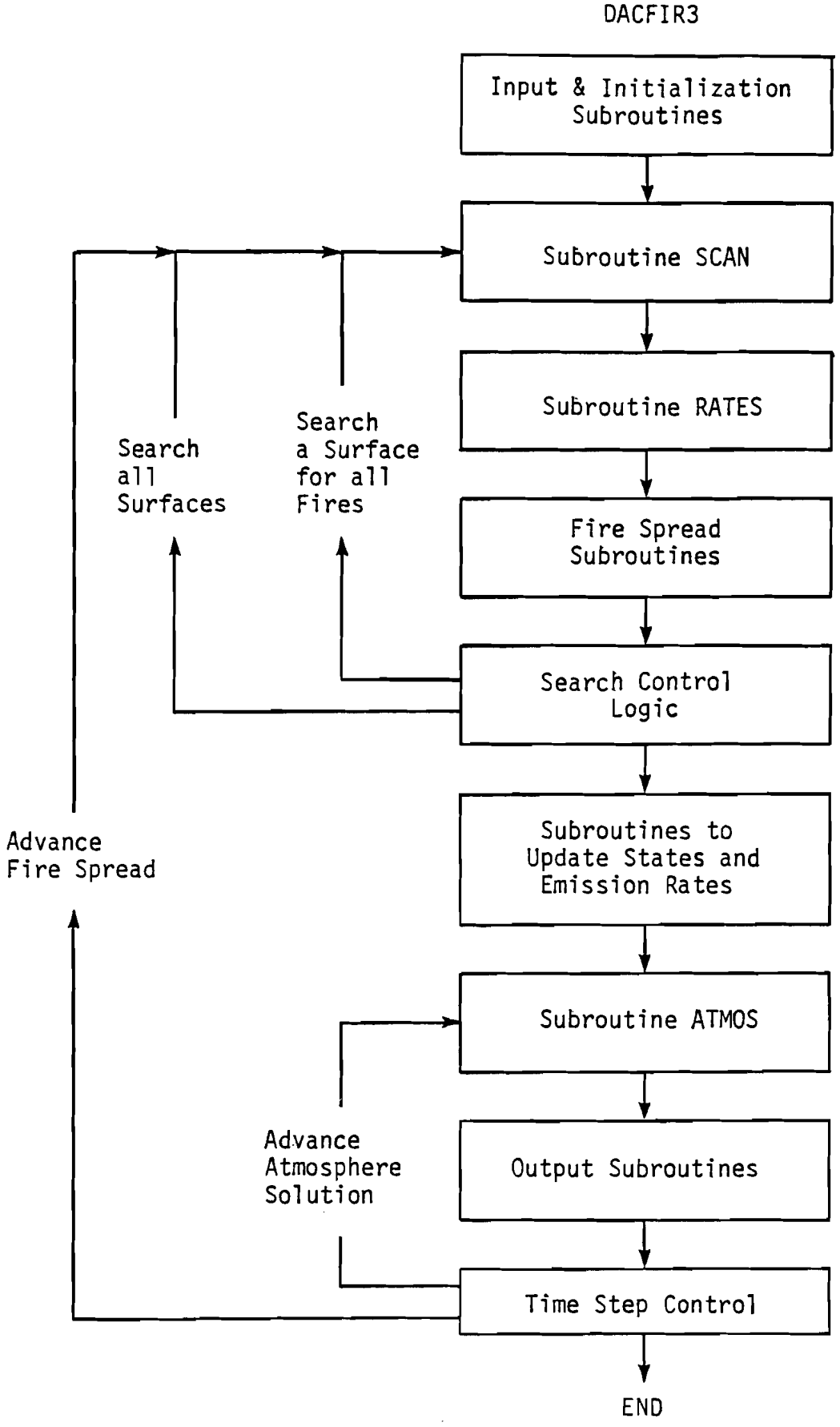

Figure 3. Organization of the DACFIR3 Program.

SECTION 3
FIRE SPREAD AND PRODUCT EMISSION

The spread of burning and smoldering over the cabin materials and the rates at which combustion products are emitted are modeled in DACFIR3 using a discrete states-transition method. This section describes the assumption and oepration of this method.

3.1 ELEMENT STATES

Each material element in the cabin is considered to be in one of seven states. The state of an element may change with time depending upon the size and location of the fire or fires in the cabin and upon the properties of the material. The seven element states are:

State 1 (Virgin)

The material comprising the element is in its virgin state; that is, it has not been directly affected by the fire or fires.

State 2 (Smoldering)

The material comprising the element is smoldering; (undergoing nonflaming decomposition).

State 3 (Flaming)

The material comprising the element is undergoing flaming combustion.

State 4 (Charred)

The material comprising the element has burned out and will no longer smolder or burn.

State 5 (Heating, no flame contact)

The material comprising the element is receiving heat flux sufficient to cause it to smolder but because of the element's thermal inertia smoldering has not yet begun.

State 6 (Heating, with flame contact)

The material comprising the element is being touched by the flames of a fire but has not yet ignited because of the element's thermal inertia.

State 7 (Smoldering and cooling)

The material element began smoldering when the heat flux to the element reached a specified level; the heat flux has now dropped below that level but the material is still smoldering. The element will continue to smolder for a specified time and then transform to the charred state (State 4).

There are two emission rates associated with each material, a smoldering rate and a flaming rate. The elements in States 2 and 7 emit smoke and toxic

gases at the smoldering rates. The elements in State 3 emit smoke, heat, and toxic gases at the flaming rate.

Element State 1 is a beginning state in which no transitions have yet occurred. State 4 is a final state from which no additional state transitions can occur. States 5 and 6 are intermediate states in the transitions to States 2 and 3. The relationship among the states is given in the transition diagram of Figure 4. The criteria governing state transitions are described in the next section.

3.2 ELEMENT STATE TRANSITIONS

An element's transition from one state to another is governed by the properties of the material and by the element's relationship to the fire or fires in the cabin. A fire is defined as a set of contiguous elements in State 3. The fire is assumed to have a flame volume whose size and radiation are a function of the area of the fire base and various properties of the fuel and the cabin atmosphere. At any time there are four sets of elements that are candidates for state transition. They are:

1. Nonburning elements adjacent to elements that are flaming. These elements are candidates for immediate ignition.
2. Elements that are inside the flame volume of a fire. All such elements are candidates for immediate ignition.
3. Elements in the general vicinity of a fire. These elements are not in danger of immediate ignition but are candidates for transition to smoldering due to the high local radiation flux.
4. Elements that are smoldering or flaming. These elements are candidates for transitions to the charred state.

The criteria for the state transitions that can occur for the elements within each of thse sets are described below.

3.2.1 Ignition by Creeping Flame Spread

The rate at which a flame front propagates over a surface depends upon several factors: the type of material at the flame edge, the size of the flames, the orientation of the surface, and the external radiation level. The flame spread rates for a given material are supplied to the model in tabular form as functions of radiation. The flux to elements adjacent to flaming elements is the sum of the radiation from the adjacent fire and the radiation from the hot gases in the upper zone. Three flame spread rates are associated with a vertical surface: vertical upward spread (f_u), vertical downward (f_d) and horizontal (f_h). One flame spread rate (f_h) is associated with horizontal surfaces. The rates and directions are shown in Figure 5.

The state of an element adjacent to a flaming element will be changed to State 3 after the original flaming element has been in State 3 for a time interval equal to or greater than d/f_i where d is the distance between the center of one element and the center of an adjacent element (six inches) and f_i is the flame spead rate in the appropriate direction for the flaming material for a given heat flux. Thus the flame front progresses in steps of

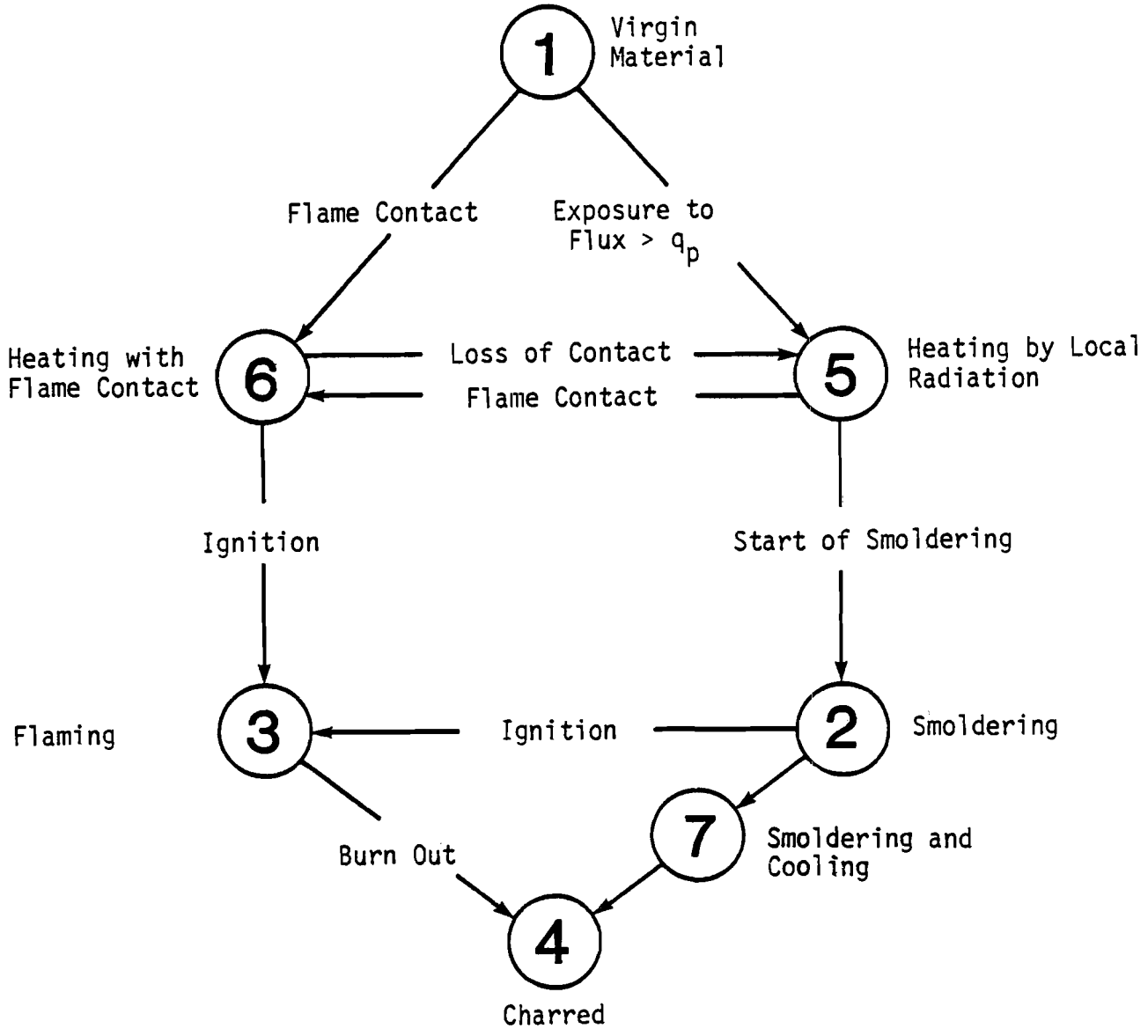

Figure 4. Element States and State Transitions.

Vertical Surface

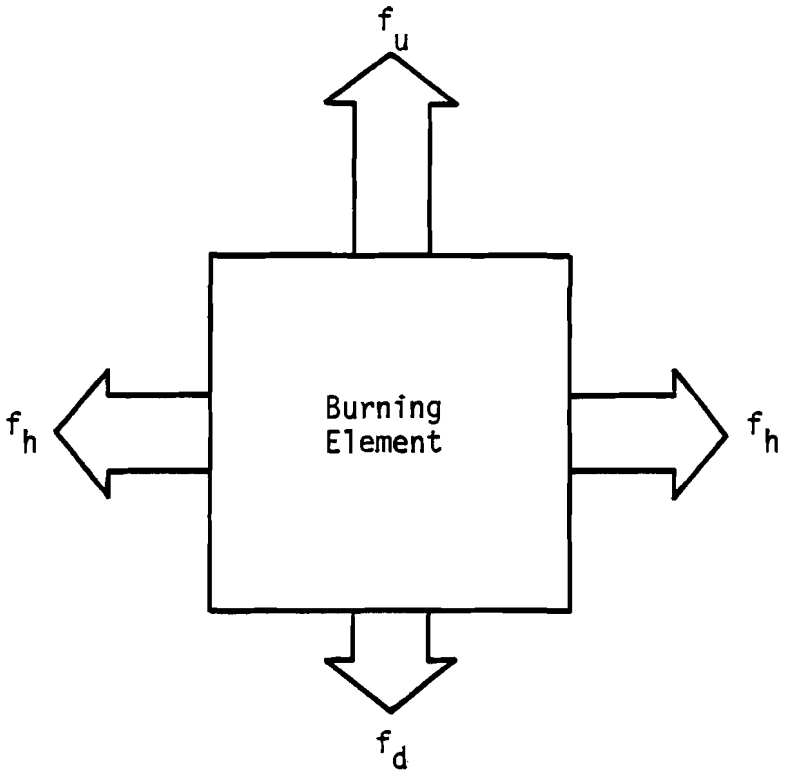

Horizontal Surface

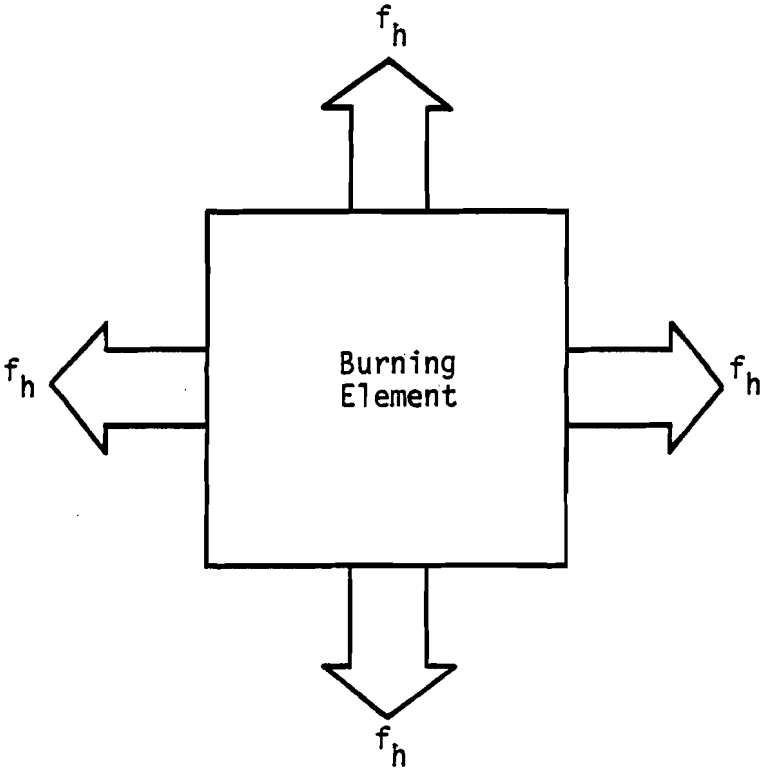

Figure 5. Flame Spread Routes for Elements on Vertical and Horizontal Surfaces.

six inches at a rate determined by the material characteristics and the radiation environment. By this process--called "creeping flame spread" to distinguish it from fire jumping across nonconnected surfaces--a fire can propagate around the interior lining of the cabin or over a seat. The fire may also propagate by this process from a seat adjacent to a sidewall to the sidewall and vice versa. A special distance and rate for this spread are supplied in the program input. If a given material will not burn, the flame spread rate can be given as zero and the fire will not propagate over the material. The fire also will not propagate to any element in State 4 (charred). The state transitions which can occur by creeping spread are all transitions to State 3 from any of States 1, 2, 5, or 6. These state transitions are shown in Figure 4.

The flame spread rates used to determine if a state transition occurs are functions of the radiation flux arriving at the material at the edge of the fire. This flux is designated as q_1 (Btu/ft^2·sec) and is computed as a function of the flame volume, emissivity, and emissive power, and of the radiation from the upper gas zone. The details of the computation of q_1 are given in Section 5.

3.2.2 Ignition by Flame Contact

The flames of a fire on one surface may touch other surfaces that are not physically connected to the surface containing the fire base. Elements on the surface in contact with the flames will eventually ignite, given sufficient exposure. In DACFIR, fires can propagate by flame contact to any surface directly above a burning element, provided that the current flame length makes contact possible. For fires originating on the vertical sidewalls, flames may contact and ignite the first row of elements on the ceiling or underside of a hatrack or passenger service unit (PSU), but no extension of the flames horizontally beneath the surface is considered.

The equation for computing the flame length is presented in Section 5. For a fire on the floor the height is, of course, measured from the floor. For fire on the sidewall the height is measured from the midpoint between the upper and lower extremes of the fire. On a seat, the height is measured from a point which is weighted average of the midpoints of four surfaces which make up the seat backrest. The weight for each surface is the number of elements on that surface in State 3 divided by the total number of elements in State 3 on the backrest.

The state transitions which occur for elements in contact with flames are:

- Elements in State 1 go to State 6
- Elements in State 2 go to State 3
- Elements in State 5 go to State 6
- Elements in State 6 go to State 3, if the element has been in State 6 longer than a time interval t_f.

The time t_f, the ignition delay for flame contact ignition, is specified in the input for each material as tabular function of heat flux. The radiation level q_2, experienced by elements within a flame volume is a function of the

same quantities as q_1 but will be of greater magnitude. The modeling of q_2 is also discussed in Section 5.

3.2.3 Transition to Smoldering

Elements in the vicinity of a fire may receive sufficient heat flux from the flames to begin smoldering. In DACFIR3, this process is allowed for elements on the floor in the vicinity of a fire on the floor, elements on the top of a seat cushion in the vicinity of a fire on the seat cushion, elements on the bottom of a seat cushion above a fire on the floor, and elements on the ceiling surfaces above a fire on a seat. Associated with each material is an input parameter, q_p, which defines the heat flux level above which the material will begin to smolder after a brief radiation exposure.

Elements on the floor in the vicinity of a fire on the floor and elements of a seat cushion in the vicinity of a fire on the cushion top will receive a heat flux level greater than or equal to q_p if they are within a distance x_p of the fire base edge. This distance is referred to as the "smoldering range" of the fire, and is found as a function of the fire radiation. The radiation flux in this case is designated as q_3. Expressions for q_3 and x_p are given in Section 5.

The following state transitions occur for elements considered to be within the smoldering range of the fire:

- Elements in State 1 are changed to State 5
- Elements in State 6 are changed to State 5
- Elements in State 5 are changed to State 2 <u>if</u> they have been in State 5 for a period greater than t_p.

The time t_p is an input parameter and is a function of the type of material comprising the element.

3.2.4 Transitions of Elements in the Smoldering or Flaming States

For each time step that an element is in State 2 (smoldering) or State 3 (flaming) a certain percentage of the total combustion products that can be emitted are emitted. For elements in State 2 this percentage is calculated by the expression

$$P_2 = (\Delta t/t_{pc})\ 100 \qquad (3\text{-}1)$$

where Δt is the length of time step and t_{pc} is an input parameter defining the total time required for the element to become charred at a heat flux of q_p. For elements in State 3, the percentage is calculated by

$$P_3 = (\Delta t/t_{fc})\ 100 \qquad (3\text{-}2)$$

where t_{fc} is an input parameter defining the total time required for the element to become charred due to flaming combustion. The parameters t_{pc} and t_{fc} are functions of the material type and heat flux. The heat flux received by a flaming element is q_2.

Each time P_2 and P_3 are calculated for an element they are added to the total percentage of decomposition, P_T, for the element. The value of P_T is initially zero and increases by P_2 or P_3 for each time period that the element is in State 2 or State 3. When P_T for an element becomes equal to or

greater than 100, the element state is changed from State 2 or State 3 to State 4, charred.

While an element is in State 2, it emits smoke and toxic gases at rates which are input to the program for each material. While an element is in State 3, it emits heat, smoke, and toxic gases at rates which are determined from an input table of these rates versus heat flux, q_2.

Elements that are in State 2 reach this state because the heat flux being received by the element is greater than q_p. If an element in State 2 is found at some later time to be outside the smoldering range of a fire, it will no longer receive a heat flux greater than q_p. In this case the element state is changed from State 2 to State 7. While in State 7 the element continues to smolder until it has been in this state for a preset time t_{pe}. The time t_{pe} is an input parameter for each material. Once the element has been in State 7 for a time t_{pe}, it stops smoldering and its state is changed from State 7 to State 4. The change to State 4 occurs even though the element is not necessarily completely consumed. Nonetheless, no other transitions are allowed for the element. Since the time period for the simulation is normally not long enough for the fire to recede from a smoldering element and lthen to grow back to it again, this approximation should be adequate for most purposes.

One other state transition is possible. An element that is within the smoldering range of a fire but has not begun to smolder (because a time interval t_p has not elapsed) is in State 5. If, due to some change in the fire condition, an element in State 5 is found to no longer be within the smoldering range of a fire, its state is reset to State 1.

All the state transitions that are possible and the characteristic time for each transition have been shown in Figure 4. The transitions depend upon the specified material parameters: three flame spread rates (f_h, f_u, f_d), five characteristic times (t_f, t_{fc}, t_p, t_{pc}, t_{pe}), and a characteristic heat flux level (q_p). The flame spread rates and the first two time constants are taken to be functions of heat flux as given in the program input.

3.3 DETAILS OF THE CABIN GEOMETRY

The cabin of a commerical transport airplane may range in size from about 10 feet in width by 50 feet in length to over 20 feet in width and more than 20 feet in length. The number of seats may range from about 90 to over 500. In the larger wide-body transports, the cabin is divided into smaller compartments by lavatories and galleys. For even the smallest cabin, the total material surface area (seats and cabin lining surfaces) exceeds 5000 square feet. All the surfaces of a cabin could be included in the grid scheme of DACFIR3 but most of the elements would never enter into the calculations. Therefore, to decrease computer time and storage requirements, DACFIR3 considers only a three-seat row-long section of the cabin for the fire spread simulation. In the time period of interest it is not likely that a survivable fire will spread beyond this region.

To describe the cabin in the input, the user of DACFIR3 need only supply a few overall dimensions of the cabin lining surfaces (i.e., the floor,

sidewalls, hatracks/stowbins, etc.) and the components of the unit vector normal to the surface. The program assembles the surfaces in the proper arrangement, divides the surfaces into the unit elements, and sets all indices and counters necessary for the fire simulation to proceed over the surfaces. All common transport category cabin interior linings can be represented by this method.

All dimensions, locations, and directions in DACFIR3 are specified in a single coordinate system. A right-handed cartesian system is used with the origin located in the forward lower right-hand corner of the cabin as viewed facing forward. This coordinate system is shown in Figure 6. The figure also shows a typical location for the "detailed section," the part of the cabin where the grid scheme is applied.

3.3.1 Cabin Lining Surfaces

The lining surfaces in an aircraft cabin include the carpet, sidewalls, window reveals and transparencies, passenger service units, stowage bins, and ceiling panels. Older aircraft may use the shelf-like hatracks instead of the stowage bins. Lining surfaces are assumed to be oriented either vertically or horizontally with respect to the floor. A maximum of 20 individual lining surfaces can be used. The vector normal to a surface is specified to identify the surface orientation and a "z displacement" is used to locate the bottom edge of the surface with respect to the cabin floor. For horizontal surfaces, the z displacement is the distance from the floor to any point on the surface (as all points are equidistant from the floor). A surface width is specified which is the surface z dimension for vertical surfaces and the x dimension for horizontal surfaces. The cabin cross section (parallel to the x-z plane) is assumed to be the same for all compartments.

3.3.2 Seats

Seat positions and seat row widths are user-definable in DACFIR3. Seats are modeled by a simple bench-like approximation. Seats side by side in a row are regarded as a single bench seat, called a seat group, whose width may be specified provided that it is an integer multiple of 0.5 feet. The other dimensions of a seat are assumed to be constant. The seat cushion is 1.5 feet from back to front; the backrest 3.5 feet high, and both cushion and backrest are 0.5 feet thick. Figure 6 shows the seat configuration and dimensions. Up to nine seat groups may be represented in the model, each with a different width if required. All seats are assumed to face forward, with the vertical backrest planes perpendicular to, and the horizontal cushion planes parallel to the floor. The location of each seat group is given by specifying the x and y coordinates of the forward right-hand corner of the seat cushion as viewed by a person sitting in the seat.

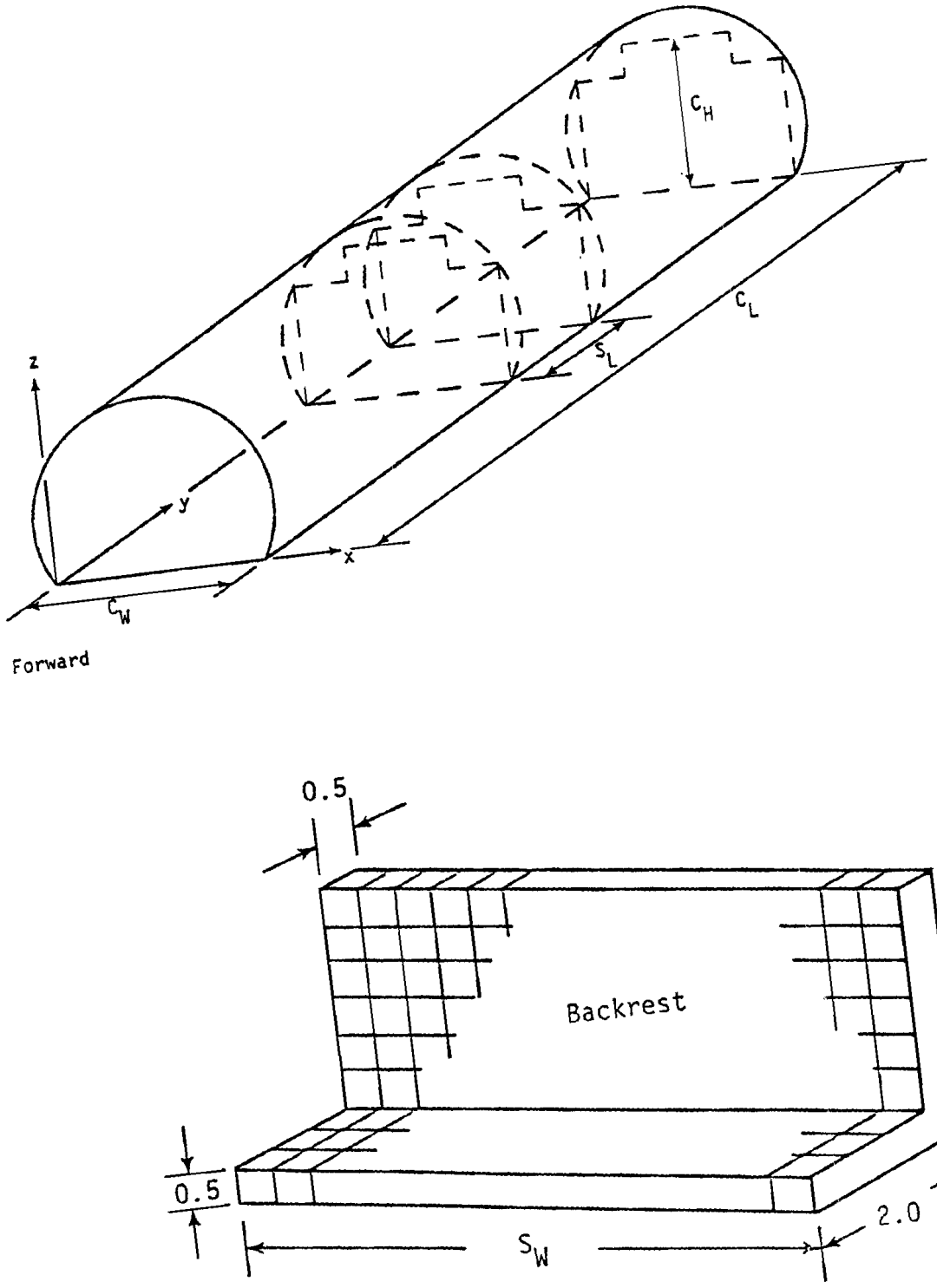

Figure 6. Cabin Coordinate System and Seat Dimensions.

SECTION 4

CABIN ATMOSPHERE MODEL

The objective of the cabin atmosphere model of DACFIR3 is to predict the changes in gas temperature and composition as the fire develops. The "two-zone" method of representing the cabin atmosphere, used in the earlier versions of DACFIR, is extended in DACFIR3 to cabins divided into several compartments. The two-zone method assumes the cabin atmosphere within a compartment to be divided into two separate horizontal regions or zones. The upper zone consists of combustion products and heated air which have risen toward the ceiling by natural buoyancy. Below this region is the lower zone consisting of cooler, denser, less contaminated air that was originally in the compartment or which enters the compartment through doors or vents. Both zones are assumed to be well mixed so that single values of temperature, smoke, and gas concentrations suffice to describe the state of each zone. Changes in the mass, composition, energy, and volume of each zone occur by the action of fires in the compartment, by radiative and convective heat exchanges between the zones and with the confining walls, and by the effects of flows in and out of vents.

This section presents the governing equations for the DACFIR3 model of the cabin atmosphere. Much of this development is similar to that previously reported for the earlier versions of the model and by others. Enough new material has been added, however, to justify a complete restatement of the physics and mathematics.

4.1 ZONE MODEL FOR MULTIPLE COMPARTMENTS

The extension of the two-zone model to multiple compartments is straightforward. Each compartment is divided into an upper and lower zone when hot combustion gases are present. Flows between compartments are driven by density and pressure differences between the zones. Figure 7 shows the interaction between two compartments including the flow from one of the compartments to the exterior. The broken lines in the figure define the control volumes for each zone. When the burning material of a fire base is located below the thermal discontinuity it is convenient to extend the upper zone control volume down through the flames and plume to the burning surface. Mass flow across the boundaries of each control volume occurs at the planes of vents and at the entraining surfaces of flames and plumes.

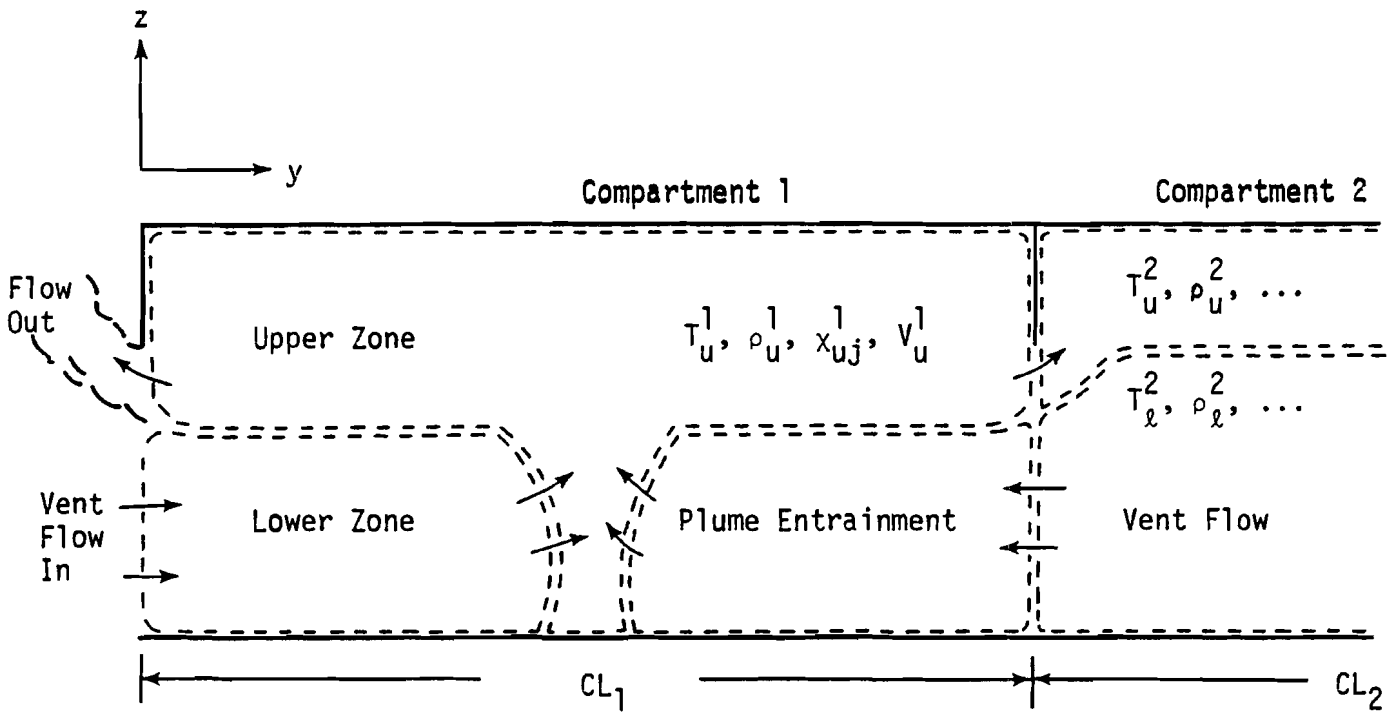

Figure 7. Gas Zone Control Volumes and Mass Flows

We make the following simplifying assumptions about the compartmentation and cabin design:

- A maximum of four compartments is allowed
- Compartments are arranged linearly along the fuselage so that no compartment is connected to more than two others
- The floor levels in all compartments are equal
- The cross-section (in the x-z plane) of all compartments is identical
- Any or all compartments may have vents (doors, escape hatches, etc.) leading to the outside or to other compartments, but no compartment has more than six vents
- The partitions dividing the compartments are vertical planes of negligible thickness.

All the above assumptions, with perhaps the exception of the last, are appropriate to any modern cabin design. We also assume that the cabin floor is horizontal so that the plane of the boundary between the zones is always parallel to it.

When DACFIR3 is used with multiple compartments, the user specifies the compartment in which the grid scheme for tracking interior fires is used. All

burning and smoldering of interior materials will be confined to this compartment and the limitations of the grid. The activity in other compartments is limited to the accumulation of combustion products by flow through vents--including the inflow of gases from an exterior fire--and the exchange of heat between zones and to the confining walls.

The equations governing the behavior of each zone in each compartment are presented in the next section.

4.2 CONSERVATION EQUATIONS

For the control volumes defining the upper and lower zones in a compartment, application of the conservation of mass, energy, and species allows us to write a set of ordinary differential equations for the mass, composition, and energy in each zone. When we add several additional relationships (the gas law, etc.) and apply the fact that the volume of each compartment is fixed, the equation set is closed and may be solved numerically for specified initial conditions.

The develoment of the conservation equations follows standard procedure and so will be given in an abbreviated form.

4.2.1 Conservation of Mass

Conservation of mass applied to both zones in a compartment yields, for the upper zone

$$\frac{d}{dt} M_u^i = \sum_{\text{vents}} G_{vu}^i + \sum_{\text{plumes}} G_p^i + \sum_{\text{fires}} G_f^i \qquad (4\text{-}1)$$

and for the lower zones

$$\frac{d}{dt} M_\ell^i = \sum_{\text{vents}} G_{v\ell}^i - \sum_{\text{plumes}} G_p^i \ . \qquad (4\text{-}2)$$

The superscript i indicates the ith compartment if more than one is used. The summations of the various mass flow rates are understood to be taken over the surface areas of each control volume through which mass passes. Thus the vent flows, G_v^i, occur only if some of the zone surface is in contact with a vent opening. The second summation on the right of both equations represents the rate of entrainment of mass into the plumes of fires whose bases extend into the lower zone. The assumed algebraic sign for all mass flows and thus for G_p is positive for flow into the control volume. Therefore the sum is positive in (4-1) and negative in (4-2). Vaporizing fuel adds mass to the upper zone across the base planes of any burning surface. This flow, small but not always negligible, adds to the right hand side of (4-1). Further analysis of each of the mass flow rates will be given in later sections.

4.2.2 Conservation of Species

In DACFIR3 we make the following assumptions about the composition of the cabin atmosphere:

- All gas consists primarily of five major species N_2, O_2, "fuel vapor," CO_2, and H_2O.
- Any additional species, e.g., CO, HCN, HCl, etc. exist at such a low concentration that the contribution to the mean molecular weight in any zone is negligible. These are the "trace species."
- Smoke is treated as a trace specie without mass but with a concentration related to its optical density.

These assumptions allow a unified and economic treatment for the computation of smoke and gas concentrations. The major species were chosen because most cabin materials are polymers of carbon, hydrogen, oxygen, and nitrogen and so might be expected to produce primarily CO_2 and H_2O upon combustion. The specific trace species and their molecular weights are defined by the user in connection with the emission rate data supplied for the materials. Concentrations of the trace species and the major species are given in terms of mass fraction, χ^i_j, of the jth specie in each zone:

$$\frac{d}{dt}(\chi^i_{uj} M^i_u) = \sum_{\text{vents}} \chi_j \, G^i_{vu} + \sum_{\text{plumes}} \chi^i_{j\ell} G_p + \sum_{\text{fires}} W^i_{jf} + \sum_{\text{smolders}} W^i_{js} \qquad (4\text{-}3)$$

and for the lower zone,

$$\frac{d}{dt}(\chi^i_{\ell j} M^i_\ell) = \sum_{\text{vents}} \chi^i_{j\ell} G^i_{v\ell} - \sum_{\text{plumes}} \chi^i_{j\ell} G^i_p \quad . \qquad (4\text{-}4)$$

The subscript j refers to the jth specie.

For the vent flow terms, some flows may be out of a zone and so will use the mass fraction of the jth specie in that particular zone. In other cases the flow will be into the zone from an adjoining compartment or from the exterior so that the mass fraction will be characteristic of the zone where the flow originates. Zone subscripts and compartment superscripts have therefore not been placed on the mass fraction variable for the vent flow terms.

Flames and plumes of fires in the lower zone entrain the species from that zone and so χ^i_{jP} appears on the right of both equations. The final two terms of (4-3) are the mass generation rates of the jth species assumed to occur at the base planes of fires and over the areas of smoldering materials. This is the point of connection between the product generation data of trace species specified for the cabin materials and the atmosphere model. The summations for the generation terms are developed in the flame spread sections of the computer code and delivered to the cabin atmosphere as a single term which applies only to the compartment containing the element grid. Although the model assumes that no plumes exist above smoldering regions in the lower zone and that no significant mass is generated by smoldering, we place all the

trace species generated by smoldering in the upper zone, since it is likely that they will rise to that area by buoyancy.

For all true chemical species, the variables χ_j are mass fractions and thus unitless. For smoke, the input generation data is in units of "particles of smoke" generated per square foot per second. The unit "particle of smoke," introduced by Smith (Reference 12) to quantify rates of smoke release, is defined as that amount of smoke which when confined to a volume of one cubic foot reduces the transmission over a one foot light path by 10 percent. Units for χ_j for smoke are then particles per lbm of mixture.

In the case of oxygen consumption, the term W_{O_2} is negative and its value is obtained from the specified values of the heat of combustion for each material, ΔH_{ck}, the total rate of heat release $\dot{Q}_k$ over all the burning area of this material, and the stochiometric oxygen-to-fuel mass ratio, γ_k, The subscript k denotes the kth material. We assume an overall stoichiometric combustion so that

$$W^i_{O_2} = - \sum_{k \text{ materials}} \gamma_k \dot{Q}_k / \Delta H_{ck} \qquad (4\text{-}5)$$

where the units of $W^i_{O_2}$ are pounds of O_2 consumed per square foot per second.

Generation rates of the major product species CO_2 and H_2O are computed from the rate of mass consumption as estimated by the ratio $\dot{Q}_k/\Delta H_{ck}$. With a specified molecular weight for each material, ω_k, the rates of production of carbon dioxide and water vapor are

$$W^i_{CO_2} = \sum_k (44/\omega_k)(\dot{Q}_k/\Delta H_{ck}) \quad , \qquad (4\text{-}6)$$

$$W^i_{H_2O} = \sum_k (18/\omega_k)(\dot{Q}_k/\Delta H_{ck}) \quad .$$

The stoichiometry assumed in this process is that mole of fuel, of whatever type, yields one mole each of CO_2 and H_2O upon combustion. [This situation would strictly apply only if all materials could be characterized by a structure $(CH_2)_n$ so that the overall reaction would be $(CH_2)_n + (3n/2)O_2 \rightarrow nCO_2 + nH_2O$.]

In DACFIR3 no unburned fuel vapor is assumed to be present in either zone so that the value of χ^i_{fuel}, for each zone is always zero. Similarly, no consumption rate term, W^i_{fuel}, analogous to $W^i_{O_2}$, is computed and the conservation equation for the fuel species involves only null arithmetic. This approach of keeping a variable and equation for fuel vapor was taken in anticipation of later refinement to include such phenomena as incomplete combustion and the accumulation of unburned hydrocarbons which may become

involved in other fires. In the same sense, there are no production or consumption terms for the lower zone species equations in this version. Consequently mass fractions in the lower zones of all compartments will not change. (This assumes all lower zones exchange flows only with one another. This assumption is discussed in the section on vent flows.) By writing species conservation equations for the lower zone we anticipate refinements to include mixing between upper and lower zones, which is known to occur but for which no model is yet available (see Reference 13).

4.2.3 Conservation of Energy

In applying the first law of thermodynamics to each zone control volume we may assume that the heat addition or loss occurs at constant pressure. There are no work interactions so the conservation of energy for the upper zone is

$$\frac{d}{dt}(M_u^i c_p T_u^i) = \sum_{\text{vents}} E\, G_{vu}^i + \sum_{\text{plumes}} c_p T_\ell^i G_p^i + \sum_{\text{fires}} \dot{Q}_f^i + \sum_{\text{surfaces}} \dot{Q}_{cvn}^i + \dot{Q}_{rin}^i - \dot{Q}_{rout}^i \tag{4-8}$$

and for the lower zone

$$\frac{d}{dt}(M_\ell^i c_p T_\ell^i) = \sum_{\text{vents}} E\, G_{v\ell}^i - \sum_{\text{plumes}} c_p T_\ell^i G_p^i + \sum_{\text{surfaces}} \dot{Q}_{cvn}^i + \dot{Q}_{rin}^i - \dot{Q}_{rout}^i \tag{4-9}$$

The first assumption to note is that we take the specific heat at constant pressure, c_p, to be independent of temperature and composition. We use the value for room temperature air, 0.24 Btu/lbm-R, throughout. As discussed for the species conservation equations, the energy transported through the vents will depend on the flow direction so that the gas temperature involved must be separately determined in each case. When the equations apply to the compartment containing interior fire, the plume entrainment (if any) will carry enthalpy from the lower zone to the upper as given by the second term on the right in each case. The third term on the right of (4-8) represents the total heat release by all interior fires since, by convention, all fire bases contact the upper zone. The convective loss to the non-burning surfaces appears as an addition, although the term is computed in a way that preserves the sense of the heat flow which is normally out of the zone. The remaining two terms are the rates of radiation absorbed by the zone gas, $\dot{Q}_{rin}^i$, and the rates of emission, $\dot{Q}_{rout}^i$. The method of computing all the energy flow terms is presented in the following sections.

4.3 INTERIOR FIRES

Fires in the compartment entrain mass, species, and energy from the lower zone into the upper zone. A number of analyses of the behavior of fires of the scale considered by DACFIR (i.e., base diameters on the order of several feet) are available in the literature. The model of Steward (Reference 14) and its its extension by Fang (Reference 15) have been chosen for use in DACFIR because it incorporates heat generation in the flames and includes the effect of reduced oxygen concentration in the entrained gas.

Steward's model was developed for fires with horizontal, circular bases and axisymmetric flame and plumes rising above the base plane. DACFIR allows fires on vertical and horizontal downward facing surfaces with base plane areas of any pattern that can be formed by connected square elements. Since we employ the fire model only to estimate the entrainment and not such items as flame temperature or velocity we adopt Steward's entrainment relationships with the understanding that better models which include all the complex geometric effects of the base shape and orientation are needed. For the fire base radius, y_o, in the Steward model we use the hydraulic radius of the base defined as

$$y_o = 2A/P \qquad (4\text{-}10)$$

where A is the base area and P is the base perimeter.

The fire structure assumed by the Steward model is shown in Figure 8. An axisymmetric column of gas rises from the burning surface, the column radius varying with height as air is entrained into the turbulent flow. Two regions in the plume are identified: the combustion zone which extends from the base to the point at which a stoichiometric mixutre is reached, and above that, the plume zone where no further reaction is assumed. We have used the term plume earlier to signify the entire gas column that is a fire, but here we reserve the term for the region of the column where there is no further heat generation. Note here that in Steward's model the stoichiometric mixture height, Z_s, and the visible flame height, h_f, do not coincide. Further discussion of this point is given below.

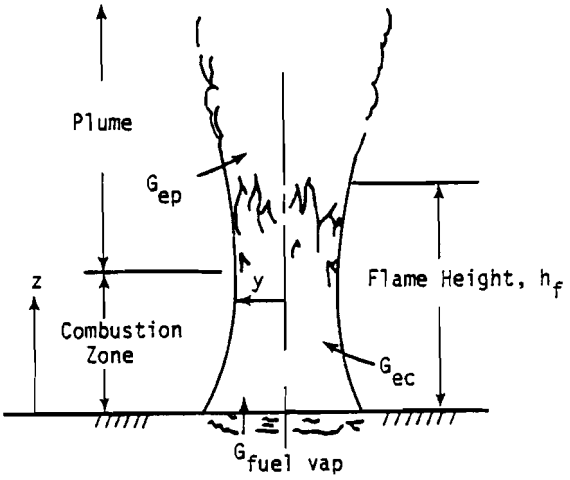

Figure 8. Fire Structure and Entrainment Flows in Steward's Fire Model.

The rate of mass flow into the combustion zone from the base to a height z is given in Steward's theory by

$$G_{ec} = Au_o\rho_\ell\omega\{[0.673\ E_c^{4/5}\omega^{-3/5}(1-\omega)^{1/5}(gy_o/u_o^2)^{1/5}z/y_o + 1]^{5/2} - 1\}. \quad (4\text{-}11)$$

where

$$\omega = [\gamma c_p T_\ell^i/(\gamma c_p T_\ell^i + \chi_{\ell O_2}^i \Delta H_c)] \ .$$

The values of u_o, γ, and ΔH_c are those for the material of the fire base. The combustion zone extends from the fire base to the stoichiometric mixing height given by

$$z_s = 1.49\ E_c^{-4/5}[\omega/(1-\omega)]^{1/5}(\omega\rho_\ell\rho_o + \gamma/\chi_{\ell O_2})^{2/5}(\rho_o u_o/\rho_a\sqrt{gy_o})^{2/5} \quad (4\text{-}12)$$

Above this point the plume entrains lower zone gas at a rate proportional to the distance above z_s given by

$$G_{ep} = A_s u_s \rho_\ell\{[1.09\ E_p^{4/5}\ (gy_s/u_s^2)^{1/5}\ (1-\rho_s/\rho_\ell)^{1/5}\ (z-z_s)/y_s + 1]^{5/3} - 1\} \quad (4\text{-}13)$$

where y_s, u_s, and ρ_s are the column radius, velocity, and density at the stoichiometric point. A_s is the column cross-sectional area πy_s^2. The values of these quantities are computed from expressions given by Fang, using the same information about the fire base and fuel vapor employed in (4-11, 12, and 13). For brevity these expressions have been placed in Appendix B of Volume II.

DACFIR3 tests for the postion of the fire base midpoint and the point of stoichiometric mixing with respect to the thermal discontinuity. The appropriate values of z are then inserted in (4-11) and (4-12 and 13) as required to find the total entrainment by this fire column. The same calculation is performed for each interior fire whose base midpoint lies below the thermal discontinuity. The sum over all the fires is the mass entrainment term of (4-1). In the energy and species equations, the mass entrainment rate is multiplied by $c_p T_\ell^i$ or the species mass fractions $\chi_{\ell j}^i$ as appropriate to find the entrainment flows of these quantities.

Two added points should be mentioned concerning the entrainment expressions. First, the values of the heats of combustion ΔH_c used in (4-11) and (4-12) are "effective" values wherein the standard heat of combustion is reduced by a given factor to account for the heat lost by flame radiation. The size of this loss is not well defined but is on the order of 30 to 40 percent for the smokey flames of polymeric materials. Since the user supplies the effective ΔH_c in the program input, no specific assumption about the radiation adjustment is made by DACFIR3. Second, the values of the entrainment constants E_c and E_p are not well defined. Estimates for the values range

from about 0.1 to as high as 0.3. The values chosen for DACFIR3 are 0.15 for E_c and 0.10 for E_p.

The Steward model is also used to compute flame length, h_f, for the fire spread computations. The flame length is not, as one might first expect, the same as the stoichiometric height z_s but is typically several times this distance. The prediction of flame length was developed by Steward by correlating the model with experiemental data or fires of a large range of sizes. Further discussion of the flame length prediction method is given in Section 5.

4.4 VENT FLOWS

DACFIR3 has two methods for dealing with the flow of gases through compartment vents. In the first method the user specifies the volume flow rate and direction at a vent. The program uses this constant "forced" flow throughout the simulation regardless of the compartment atmosphere conditions. Forced flow is used when the model is to be compared to the results of tests which employ forced ventilation. It is also used in the special case of an exterior fire at the vent. In this case the temperature and composition of the inflowing fire gas must also be given in the input.

In the second method, the program computes the flow rate using the compartment pressure and the buoyancy of the hot gas. This "free" flow situation is that which would normally occur at cabin exit doors and between compartments in a post-crash fire. The method for buoyancy driven flow from a single compartment to the exterior single compartment to the exterior is now a standard technique verified by a number of experiments. Extensions of the method to the flow between two compartments, both containing layers of hot gas, were made by Tanaka (Reference 16) and by Emmons (Reference 17). The extensions involve no new physical assumptions but require a complicated switching structure to account for all the flow situations that can occur. The application of the free-flow computations to multiple compartments in DACFIR3 is essentially Emmons' formulation but with a different logical structure to account for all possible flow cases.

Figure 9(a) shows a single compartment with a buoyant flow of hot gases to the outside and a cold return flow through the lower part of the vent. In part (b) of the figure the interior and exterior pressures are shown as functions of height above the floor. The curves are given by the hydrostatic law for constant density gas in each zone. The rate of pressure change with height in the interior decreases less rapidly above the thermal discontinuity height, z_d, since the density in the upper zone is less than that in the lower zone. In the example of Figure 9 (a) and (b), the lower zone temperature and density are equal to the outside values so that the slope of the pressure curve in the lower zone is the same as the slope outside. The pressure in the lower zone, however, is lower at every height than the outside

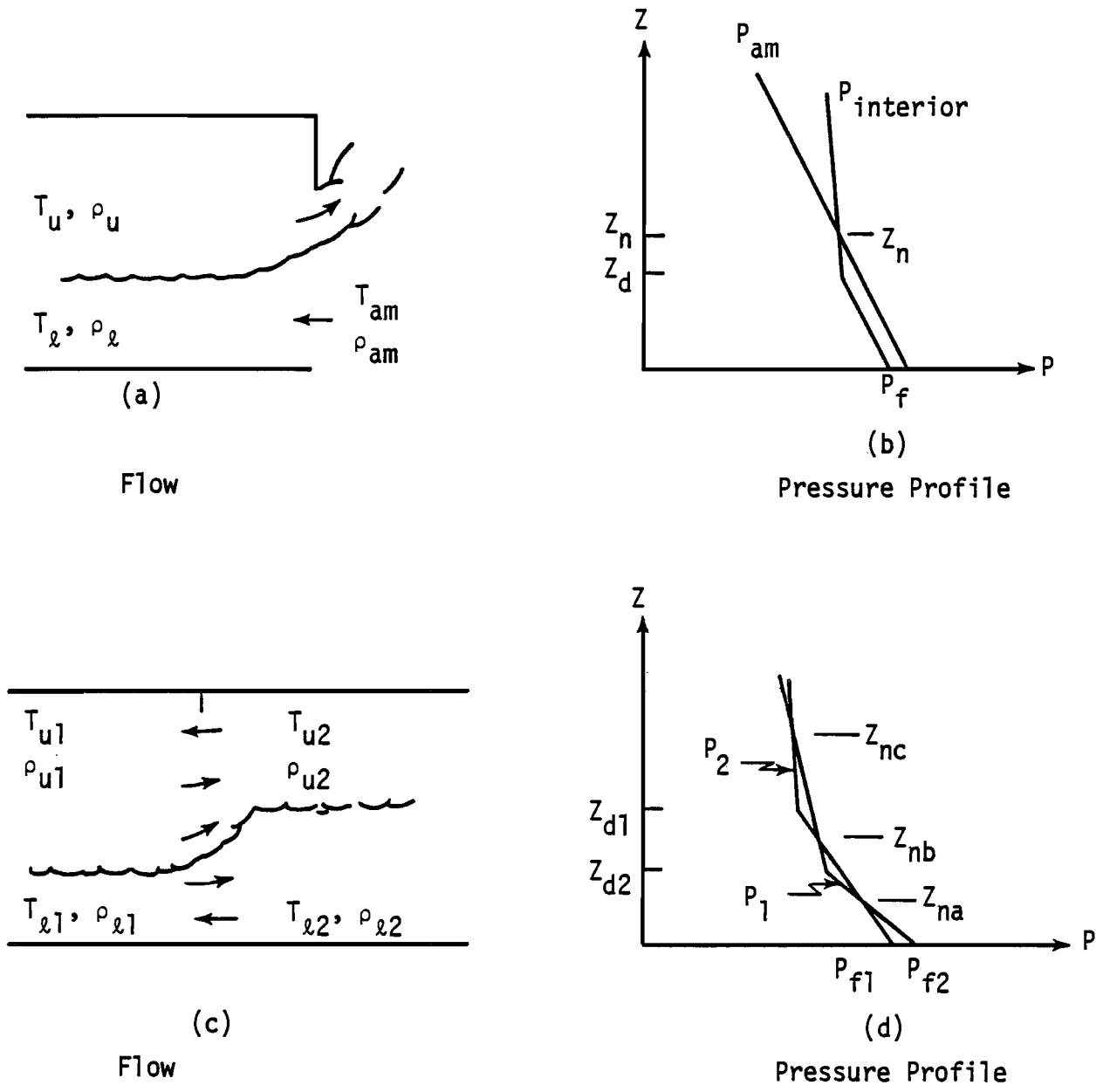

(a) & (b) Single Compartment Flow to Exterior
(c) & (d) Flow Between Two Compartments

Figure 9. Pressure and Buoyancy Driven Flows Through Compartment Vents.

pressure because of the entrainment of lower zone gas by fire plumes inside. This results in a lower interior pressure at the floor, P_f, than the outside pressure at the same level. The point at which the pressure profiles cross is called the neutral axis, z_n, which defines the boundary between the flows in the vent plane.

To compute the flow rates for this situation, the Bernoulli equation is used to express the gas velocity at the vent plane in terms of the pressure difference between the inside and outside. The product of the velocity and density of the flowing gas is the mass flow rate per unit area as a function of height. Since the pressure difference is a piecewise linear function of z, analytic forms can be found for the integrals of the mass flow rates for each section of the pressure difference function. The flow rates are corrected in the usual way by use of an empirical orifice coefficient. The mathematical details of this procedure are given below in the specific case of the flow between two compartments.

The flow between two compartments can result in a more complicated situation as shown in Figures 9(c) and (d). Both compartments contain two zones and the pressure at the floor may differ between compartments. The particular values of the four densities involved and the location of the two-zone boundaries, z_{d1} and z_{d2}, may result in three separate neutral axes, z_{na}, z_{nb}, and z_{nc} as shown. As in the more simple case of 9(a) and (b), the method of computing the flow rates involves writing the mass flux as a function of the piecewise linear pressure-height relationship. Integration over z from the bottom to the top of the vent gives the mass flows. In the case shown in 9(c) four separate flows occur.

The mathematical procedure for computing the flows between the compartments is as follows. The hydrostatic law applied to each compartment (numbered 1 and 2) gives pressure as a function of z as

$$P_1(z) = P_{f1} - \rho_{\ell 1} g z \quad , \quad z \leq z_{d1}, \tag{4-14a}$$

$$P_1(z) = P_{f1} + g(\rho_{u1} - \rho_{\ell 1}) z_{d1} - \rho_{u1} g z \quad , \quad z > z_{d1}, \tag{4-14b}$$

$$P_2(z) = P_{f2} - \rho_{\ell 2} g z \quad , \quad z \leq z_{d2}, \tag{4-15a}$$

$$P_2(z) = P_{f2} + g(\rho_{u2} - \rho_{\ell 2}) z_{d2} - \rho_{u2} g z \quad , \quad z > z_{d2}. \tag{4-15b}$$

Depending on the values of P_{f1}, P_{f2}, the four densities, and the two thermal discontinuity heights, one to three neutral axes may exist or there may be no neutral axes. In the latter case, the flow will either be all into or all out of the vent.

To find the neutral axes, if any, DACFIR3 solves for the intersections of each of the lines represented by equations (4-14) with each of the lines given by (4-15). This results in four "candidate" axis heights z_i, one or more of which is not physically possible. The case where the upper- or lower-zone densities are equal in both compartments and thus the pressure profiles are parallel is recognized in a "dummy" intersection height of a negative value is set. The set of four candidate axis positions is tested for physically incorrect values--that is, any negative value (axis below floor level) or any intersection on the wrong side of the thermal discontinuity. For example, the profile of the upper zone pressure in compartment 1 could

intersect the profile of the lower zone pressure of compartment 2 at a value of z less than z_{d1}, but since the upper zone of 1 does exist below z_{d1} there is not a neutral axis at this point.

As the neutral axes are identified they are combined in a list with the one or two z_d's. When the list is complete it is sorted into increasing numerical order. The upper and lower edges of the vent opening are then placed in the list and any z_d or z_n not in the vent opening is removed. What remains then is an ordered list of the breaks in the piecevise linear curve of pressure difference between the compartments versus z for values of z in the vent opening. Symbolically, this function is

$$\begin{aligned} z_0 \leq z < z_1, &\qquad \Delta P = f_1(z) \\ z_1 \leq z < z_2, &\qquad \Delta P = f_2(z) \\ \vdots &\qquad \vdots \\ z_{n-1} \leq z < z_n, &\qquad \Delta P = f_n(z) \end{aligned} \tag{4-16}$$

The functions f_i are either constants when the densities on either side of vent are equal or linear functions of z when the densities are not.

For the case where ΔP is constant, application of the Bernoulli equation gives

$$G_k = \sqrt{2}\, C \Delta x (\rho \Delta P)^{1/2} (z_k - z_{k-1}) \tag{4-17}$$

where G_k is the mass flow rate through the vent between the heights z_{k-1} and z_k, Δx is the vent width, and C is an orifice coefficient, taken as 0.68 in all cases. The value of ρ, the density of the flowing gas, is determined from the sign of ΔP and the zone from which the gas flows. Equation (4-17) is also used in the special case when ΔP is equal to zero.

When ΔP is a function of z the mass flow rate between z_{k-1} and z_k is

$$G_k = (2\sqrt{2}/3) C \Delta x\, \rho^{1/2}\, (1/a)[(\Delta P_{z_k})^{3/2} - (\Delta P(z_{k-1}))^{3/2}], \tag{4-18}$$

where

$$a \equiv [\Delta P(z_k) - \Delta P(z_{k-1})]/(z_k - z_{k-1}).$$

As in (4-17) the specific value for ρ and the algebraic sign of G_k depends upon the sign of the pressure difference between the compartments. The development of the list of break points z_k ensures that $\Delta P(z_k)$ and $\Delta P(z_{k-1})$ have the same sign (in some cases one of the values may be zero) so that the choice of flow direction and density is unambiguous.

When all mass flows between the break points z_k have been found they are summed into four categories depending upon the origin zone and destination zone of each flow. We make the following assumptions about the behavior of the flows: hot gases from upper zones flow only to adjacent upper zones and cold gases from lower zones flow only to adjacent lower zones. Between compartments 1 and 2 there are then four possible net flow rates; from the upper zone of 1 to that of 2, from the upper zone of 2 to that of 1, and the analogous pair for the lower zones. The various G_k's are summed into these

four categories and the corresponding flows of energy (heat) and species are found by multiplying the G_k's by the appropriate values of c_pT and χ_j and summing.

The above process is carried out for every vent in the compartment or compartments at each time step. The program logic is constructed so that no vent need be considered more than once.

Two special situations should be noted. First, when the vent is open to the outside the procedure outlined above is applied by assuming the exterior to be another compartment whose lower zone always covers the vent. The pressure at floor level in this "outside" compartment is always fixed at the user specified ambient value. Similarly, the outside temperature and density are set to fixed values in the input. The program keeps a fixed thermal discontinuity height for the outside as a large value, much greater than the top of any vent.

The other special situation is the case of an exterior fire at a vent. Here the user specifies the volume inflow rate of exterior fire gas, $\dot{V}_{exf}$; and the temperature, density, and composition of the gas, T_{exf}, ρ_{exf}, and χ_{jexf}. These values are fixed throughout the run irrespective of what conditions develop in the interior. The mass inflow rate is then $G_{exf} = \rho_{exf}\dot{V}_{exf}$ and the energy and species flows are $c_pT_{exf}G_{exf}$ and $\chi_{jexf}G_{exf}$.

4.5 CONVECTION AND RADIATION

Gases in both the upper and lower zones of each compartment may exchange heat with the confining surfaces of the cabin and with the neighboring zone. DACFIR3 incorporates the following heat transfer mechanisms:

- Convective heat transfer between the cabin lining surfaces and the gas in both zones.
- Radiation from the hot upper zone gas to all cabin lining materials.
- Radiation to each zone from the surfaces in contact with that zone.
- Radiation between zones.

The other possible radiative patterns such as the radiation from one interior surface to another are assumed to be insignificant and are ignored. DACFIR3 does not use the seat surfaces in any radiation or convective heat exchange.

4.5.1 Convection

The convective heat transfer is modeled by assuming a constant convection coefficient typical of turbulent forced convection of air at moderate velocity over a flat plate, $h = 5.5 \times 10^{-4}$ Btu/(ft^2-s-R). This value should only be regarded as a rough average because of the well known variability of h with many factors (surface orientation, flow regime, fluid properties, etc.) The heat transfer between a cabin surface at temperature T_s and a gas zone at temperature T_g is then

$$\dot{Q}^i_{cvn} = hA_s(T_s - T_g) \qquad (4\text{-}19)$$

where A_s is the area of contact between the surface and the gas zone. The model computes the fraction of each lining surface in contact with each zone. When a surface is in contact with both the upper and lower zones two surface temperatures are used, one for each section of contact. These temperatureas are independent since no lateral heat conduction within the surface material is assumed. The method of computing surface temperature is presented in Section 4.8.

4.5.2 Radiation

The radiation budget for the gas zone is the difference between the absorbed and emitted radiation. To compute the radiation emitted by a zone the following assumptions are made:

- Each zone emits and absorbs radiation as a gray gas with and absorption coefficient which is proportional to the smoke concentration.
- A mean beam length treatment is used to compute the emissivity of each zone.

These approximations were adoped by Quintiere for a two-zone model of room fires (Reference 18). The emissivity of a zone is

$$\varepsilon = 1 - \exp[-(\sigma_s \chi^i_{smk} \rho + k_g)L] \qquad (4\text{-}20)$$

where σ_s is the proportionality factor which when multiplied by the zone smoke concentration, x^i_{smk}, and density, ρ, yields an absorption coefficient representitive of the absorption and emission by the smoke. In the units of smoke opacity, employed by DACFIR3, σ_s has the value 0.1054 ft^2/particle. The absorption coefficient k_g is an added factor to correct for gas band radiation as suggested by Quintiere. The suggested value of 0.1 ft^{-1} is used for k_g.

The mean beam length, L, is estimated by the standard method for gas volumes of a rectangular shape.

$$L = 3.6 \text{ (Zone Volume}/A_{surf}) \qquad (4\text{-}21)$$

where A_{surf} is the surface area of the zone volume.

Total radiation emitted by a gas zone is given by

$$\dot{Q}_{rout} = \varepsilon A_{surf} \sigma T_g^4 \qquad (4\text{-}22)$$

where T_g is the zone gas temperature and σ is the Stefan-Boltzmann constant (4.761×10^{-13} Btu/ft^2-sec-R.) The zone also absorbs radiation from the cabin surfaces in contact with it and from the other zone in the compartment through the thermal discontinuity plane. This absorbed radiation is computed by

$$\dot{Q}_{rin} = \varepsilon\sigma\Big(\sum_{surfaces} A_{sm} T_s^4 + \varepsilon_n A_{td} T_{nz}^4\Big) \qquad (4\text{-}23)$$

where the summation is over all cabin lining surfaces in contact with the zone

gas, A_{sm} is the area of contact, and T_s is the materials surface temperature. The radiation from the neighboring zone is a function of the neighboring zone's emissivity, ε_n, and temperature T_{nz}, and the area of the thermal discontinuity plane, A_{td}. Note that the cabin surface materials are assumed to have an emissivity of unity.

4.6 GAS LAW

The pressure, temperature, density, and composition of the gas in each zone are related in DACFIR3 by the ideal gas law. An important simplifying approximation in the modeling of enclosed fires by the zone method comes from the observation that the hydrostatic variation in pressure between the floor and ceiling of compartment is small compared to the absolute pressure. This is true even when the compartment contains a layer of very hot gas. Because the change in pressure with height is small compared to the total pressure, we may ignore this variation and use a single reference pressure value in the gas law for both zones. In DACFIR3 we choose the reference pressure to be the at the compartment floor, P_f^i. Under the assumption that all compartment floor levels are the same, the reference pressure is then at the same geometric height in all compartments. Further discussion of this approximation for pressure may be found in Quintiere (Reference 13).

By assumption, only the five major gas species affect the mean molecular weight of the zone gas. Thus, the gas law for each zone in the ith compartment is written

$$P_f^i = \rho_g^i \bar{R} T_g^i \Big/ \sum_{j=1}^{5} \chi_j^i W_{mj} \qquad (4\text{-}24)$$

where ρ_g^i and T_g^i are the zone gas density and temperature, $\bar{R}$ is the universal gas constant (1545.0 ft-lbf/lbmole-R), χ_j^i is the mass fraction of the jth major gas, and W_{mj} is the molecular weight of the jth gas species.

4.7 ZONE VOLUMES AND THE THERMAL DISCONTINUITY

The position of the thermal discontinuity is determined from the fact that the total volume of each compartment must remain fixed. Thus the sum of the upper and lower zone volumes must equal a constant,

$$V_t^i = V_u^i + V_\ell^i = \text{constant} \quad . \qquad (4\text{-}25)$$

Since the cabin cross sectional area is fixed, the thermal discontinuity height, z_d^i, is a function of only V_ℓ^i

$$z_d^i = f(V_\ell^i). \qquad (4\text{-}26)$$

The form of the function f depends upon the particular shape of the cabin cross section. For example, if the cross section is a simple rectangle of width C_w and height C_h (4-26) becomes

$$z_d^i = V_\ell^i/(C_h^i C_w) \tag{4-27}$$

where C_h^i is the compartment length. If, on the other hand, the cross section is not rectangular but contains "steps" as in Figure 2, the function may not have a convenient closed-form representation. In this case, an implicit evaluation of (4-26) is employed wherein an estimate for z_d^i is used with the cabin cross section profile to compute a trial value of V_ℓ^i. The trial value is compared to the current true value which is known from (4-25). An iterative correction scheme is used to adjust the estimate of z_d^i until it results in a computed V_ℓ^i with 0.1 percent of the true value. Further discussion procedure for solving all of the cabin atmosphere equations is given in Section 4.9.

4.8 MATERIALS SURFACE TEMPERATURE

Hot gases and radiation will heat the surfaces of the cabin materials, especially those in contact with the upper zone. The upper heated surfaces then cut down the heat losses from the upper zone gas while those in contact with the lower zone will heat the lower zone gas. DACFIR3 computes the surface temperatures of the cabin lining materials: sidewalls, ceiling panels, floor coverings, etc. These structures generally consist of one or more lightweight layers of polymeric material backed by thermal insulation. Since the layers are thin, a lumped thermal model should be an adequate approximation for their temperature behavior.

Each part of the cabin lining is considered to be a sheet of thickness Δs, density ρ_m, and heat capacity c_m. The total surface area of each of these sheets is fixed and the fraction of that surface area in contact with each gas zone is computed at every integration step in the program. The important heat transfer mechanisms are taken to be convection to the zone gas, incoming and emitted radiation at the inside (cabin interior) surface and conduction through the sheet rear face in contact with the insulation layer.

The first law applied to a unit area of a cabin lining material yields

$$c_m \rho_m \Delta s \frac{dT_s}{dt} = \dot{q}''_{rin} - \dot{q}''_{rout} + h(T_g - T_s) - \frac{k_{in}}{s_{in}}(T_s - T_\infty) \tag{4-28}$$

where T_s is the materials surface temperature (assumed to be uniform throughout the sheet thickness Δs), $\dot{q}''_{rin}$ is the incoming thermal radiation, $\dot{q}''_{rout}$ is the emitted radiation by the surface, T_g is the gas temperature, k_{in} is the insualtion thermal conductivity, and s_{in} is the insulation

thickness. The insulation is assumed to be a simple linear thermal resistance of negligible heat capacity. Its outside is assumed to always be at the ambient temperature, T_∞. The incoming thermal radiation is that emitted by both gas zones, as discussed in Section 4.5.2, while that emitted by the surface is $\dot{q}''_{rout} = \sigma T_s^4$. The values of k_{in} and s_{in} are supplied by the user for each lining service.

4.9 NUMERICAL SOLUTION OF THE ATMOSPHERE EQUATIONS

Equations (4-1) and (4-2) give the rate of change of the mass of gas in each zone of each compartment, M_u^i and M_ℓ^i respectively. The amounts of mass are not as convenient to work with as are the zone densities given by

$$\rho_\ell^i = M_\ell^i / V_\ell^i \quad , \tag{4-29}$$

$$\rho_u^i = M_u^i / V_u^i \quad . \tag{4-30}$$

With these relationships the model of the cabin atmosphere is complete. Table 2 summarizes the dependent variables of the model and the primary equations which relate them. Briefly, the equations employed are the conservation relationships for mass, species, energy, and total compartment volume; the gas law for both zones; conservation of energy for the materials; the definition of density; and the geometric relationship of the boundary between the zones to the lower zone volume and cabin cross section. All the symbols in Table 2 carry the superscript i to indicate values for the ith compartment. When more than one compartment is present there is a set of (8+j+k) variables and (8+j+k) equations for each compartment. The entire set of i · (8+j+k) equations is coupled by the flows through the vents connecting compartments.

The numerical solution of this large set of mixed algebraic and ordinary differential equations poses a formidable problem. The earlier versions of DACFIR used simple one-step Euler integration for the differential equations with the necessary algebraic relationships applied explicitly where appropriate. While this method was simple and straightforward, the time steps required for a stable solution were very small, on the order of 0.001 second. The non-linear character of the equations, particularly the set used in Version 2 to compute flow through vents, made the numerical solution marginally stable at even the smallest step sizes.

A superior method for this problem is the implicit trapezoidal rule integration used by Emmons, Mitler, and Trefethen (Reference 19) for the Harvard Computer Fire Code. This method is well explained in the reference so that only a brief summary need be given here.

Each of the differential equations of the governing set can be written as

$$\frac{d}{dt} x_n = f(\{x\}) \tag{4-31}$$

TABLE 2

SUMMARY OF VARIABLES AND EQUATIONS OF THE CABIN ATMOSPHERE MODEL

Variable	Symbol	Obtained from Equation(s)
Lower zone species mass fractions (j values)*	$x^i_{\ell j}$	(4-3) (j equations) and (4-1)
Upper zone species mass fractions (j values)	x^i_{uj}	(4-4) (j equations) and (4-2)
Pressure	P^i_f	(4-24)
Lower zone density	ρ^i_ℓ	(4-29) and (4-1)
Upper zone density	ρ^i_u	(4-30) and (4-2)
Lower zone temperature	T^i_ℓ	(4-8) and (4-2)
Upper zone Temperature	T^i_u	(4-9) and (4-1)
Lower zone volume	V^i_ℓ	(4-25)
Upper zone volume	V^i_u	(4-24) and (4-30)
Thermal discontinuity position	z^i_d	(4-26)
Materials surface temperature	T^i_{sk}	(4-28) (k equations)**

* Minimum value of j is 5 and the maximum 11
** Minimum value of k is 6 and the maximum 22 per compartment

where x_n is one of the set {x} of dependent variables. In the trapazoidal rule integration, the value of x_n at time t+Δt is estimated by the formula

$$x_n(t+\Delta t) \simeq x_n(t) + 1/2[f(t) + f(t+\Delta t)] \qquad (4\text{-}32)$$

Equation (4-32) is an implicit relation for $x_n(t+\Delta t)$ since $f(t+\Delta t)$ involves the specification of the set {x} at t+Δt. When the equations represented by (4-32) are combined with the original algebraic equations the problem of predicting the values of the variables at t+Δt from the values at t becomes that of solving a large set of non-linear algebraic equations.

A number of methods are available to solve non-linear algebraic equations, each with its particular advantages and drawbacks. For DACFIR3 we have chosen the Newton-Raphson method because of its general reliability. The Newton-Raphson method is an iterative technique in which an initial guess for the solution {x} at t+Δt is repeatedly corrected using the equation set {f}. Each new correction (iteration) produces a new estimate, $\{x\}_{k+1}$, of the solution. When the (k+1) solution is sufficiently close to the previous solution, k, the set is considered solved. The closeness of two solution sets is judged by testing the difference between the corresponding values in the two sets against a pre-set tolerance.

The algorithm of the Newton-Raphson method involves writing Equation (4-32) as

$$\{x(t+\Delta t)\} = \{g(\{x(t+\Delta t)\}, \{x(t)\})\}, \qquad (4\text{-}33)$$

where the brace notation is used to indicate the complete system of n equations. The set of n functions g involve the variables at t and t+Δt. A simple rearrangement of (4-33) and the definition of another function, F, as $F_n \equiv g_n - x_n(t+\Delta t)$ gives

$$\{F(\{x(t+\Delta t)\}, \{x(t)\})\} = 0 \quad . \qquad (4\text{-}34)$$

Each of the n functions F is identically zero when x(t+Δt) solves the equation set. Since the values of x at time t are known and do not change during the iteration, we may regard the set {F} as functions only of the estimates of x at t+Δt, that is, during one time step we wish to solve for {x} such that

$$\{F(\{x\})\} = 0 \qquad (4\text{-}35)$$

where it is now understood that {x} is evaluated at t+Δt.

The equation for generating each successive estimate of the solution is

$$\{x\}_{k+1} = \{x\}_k - [J]^{-1}\{F(\{x\}_k)\} \qquad (4\text{-}36)$$

where [J] is the n-by-n Jacobian matrix of the set F. Each element of the Jacobian matrix is defined as

$$J_{ij} = \frac{\partial F_i}{\partial x_j} \quad .$$

Following the method used by Emmons, et al., the elements of the Jacobian are evaluated numerically from the definition of the partial derivative,

$$J_{ij} \simeq \frac{F_i(x_j+h) - F_i(x_j)}{h} \quad , \tag{4-38}$$

where h is a small quantity added to the jth variable of the set {x} while the other members of the set are held fixed.

Finally to solve (4-36) for $\{x\}_{k+1}$, we can rearrange once more to obtain

$$[J](\{x\}_k - \{x\}_{k+1}) = \{F\} \quad . \tag{4-39}$$

This way of writing the correction equation allows us the use of standard pre-tested computer routines for solving systems of linear equations.

The numerical technique described above is best accomplished when all the variables are of about the same order of magnitude, say on the order of one. In DACFIR3 a scaling procedure is adopted from (Reference 19) which scales the variables to O(1) before the evaluation of the Jacobian and the solution of (4-39). The new guess at the solution can then be compared to the previous guess, also given in scaled magnitude, using the same tolerance for the difference between each pair of variables. If further iteration is needed the variables are rescaled back to their physical magnitudes for the evaluation of the functions {F}.

One last point concerning the numerical solution is that the variables and equations for the cabin lining surface temperatures are not included in the iterative procedure. The thermal inertia of the materials is large enough to keep the derivatives on the left in (4-25) small during a time approximation to keep the surface temperatures constant during the iterative time step is reached, update the surface temperatures by single step Euler integration. This approximation removes from six to 20 variables and equations for every compartment--obviously a significant simplification.

SECTION 5
RADIATION

Thermal radiation to the fuel surface is the single governing parameter for determining ignition, flame spreading, product emission rates, and duration of burning for the cabin materials. The total incoming radiation at an element's surface is taken to consist of two parts: that from nearby flames, and that from the hot combustion products which form the upper gas zone. We term the first part the local flame radiation and the second part the gas zone radiation. Local flame radiation is computed by making a number of simplifying assumptions about flame structure, radiation temperature, and optical properties. This development is given in Section 5.1 below. Gas zone radiation has been discussed above in Section 4.5 where the net radiation balances for the gas control volume were given. In Section 5.2 we show how the zone radiation to a material element is estimated from the zone emittance and the element position.

5.1 FLAME RADIATION

Three estimates of the radiation from the flames of a fire are made by DACFIR3, each for a separate purpose. The flux to elements just outside of, but adjacent to, the fire base area is q_1, the average flux to elements forming the fire base area is q_2, and the flux to elements outside but in the vicinity of the tip of the flames is q_3. All these fluxes are given in units of $Btu/ft^2 \cdot sec$. Figure 10 illustrates these three quantities.

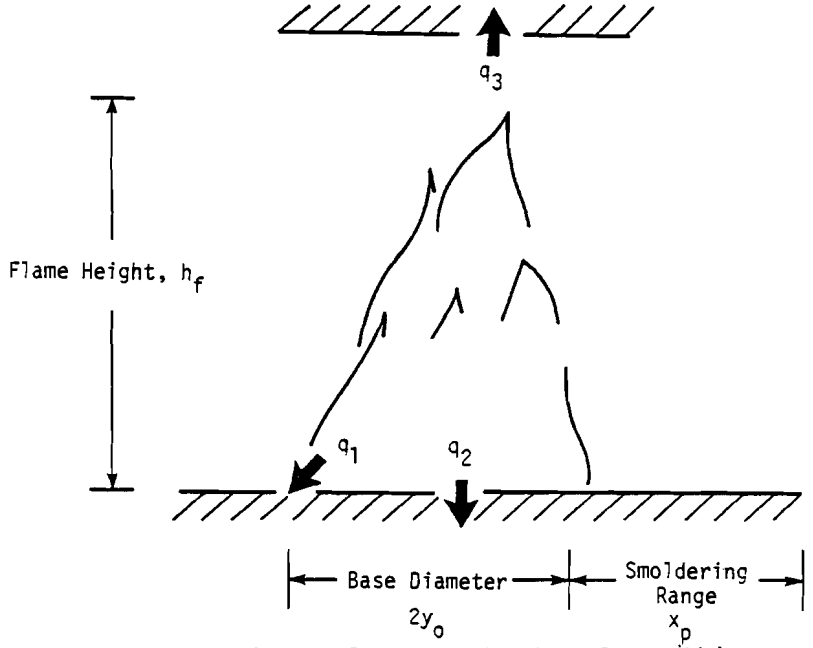

Figure 10. Flame Radiation Quantities.

To compute the radiation fluxes, the following assumptions are made about the flames:

- The flame volume may be approximated as a right circular cylinder of height h_f and base diameter $2y_o$.
- The flame volume radiates as a gray gas with a spatially uniform temperature and absorption coefficient.

For sooty flames, the type expected in cabin fires, practically all of the radiation is due to the soot pa ticles in the flame. Since measurements of the smoke generated by the cabin materials are available, the emissivities of fires of these materials can be estimated from the smoke generation data. Under a number of simplifying assumptions a method was developed to express the absorption coefficient in terms of the smoke generation rate as

$$k_f = 0.21\dot{p}'' \, (h_f g)^{-1/2} \tag{5-1}$$

where k_f is the flame absorption coefficient (ft^{-1}), and $\dot{p}''$ is the smoke generation rate of the fuel (particles/ft^2 · sec). The derivation of equation (5-1) is given in Appendix D of Reference 2. Using this estimate of the flame absorption coefficient, the emittance at the fire base center is

$$\alpha_c = [1 - \exp(-1.8k_f h_f)] + [1 - \exp(-1.8k_f y_o)] - \{1 - \exp[-1.8k_f(h_f^2 + y_o^2)^{1/2}]\}. \tag{5-2}$$

where y_o is the flame cylinder base radius (ft). This expression was developed by Dayan and Tien (Reference 20) for a cylindrical flame.

Dayan and Tien's analysis shows that the radiation flux at the edge of the flame base is about one half of the value at the base center for flames with a height-to-diameter ratio on the order of two. Since this is a typical value for the flame lengths of cabin materials we express q_1 as

$$q_1 = 0.5\alpha_c e_b \ . \tag{5-3}$$

The flame emissive power, e_b, is taken to be a constant for all fires. A study by Fu (Reference 21) of the radiation from aircraft fuel fires of base diameters of several feet indicates that the effective emissive power for these fires is about 16.3 Btu/ft^2 · sec. A review of data on smaller scale fires (about 1 ft base diameter) of plastic materials by deRis (Reference 10) shows that the emissive power of these flames is in the range of 10 to 25 Btu/ft^2 · sec. In view of this, the value 16.3 is used for e_b in DACFIR3.

For q_2, the average flux over the base, the analysis of Dayan and Tien indicates that the average vaue is approximately 84 percent of the value at the center. Therefore we write q_2 as

$$q_2 = 0.84\alpha_c e_b \ . \tag{5-4}$$

The heat flux to an element on a surface above a fire is estimated as

$$q_3 = 1/2[1 - (4\zeta^2 - 3)/\sqrt{(4\zeta^2 + 9)(4\zeta^2 + 1)}]e_b \ . \qquad (5\text{-}5)$$

This expression is obtained by using the circular cylinder model of the flame and taking the target element to be located a distance z above the tip and one-half the radius (y_o) from the axis of the cylinder. The ration z/y_o is the factor ζ of (5-5).

The smoldering range x_p, is the distance away from the flame foot at which the radiation drops to the level q_p. To compute x_p we again employ the analysis of Dayan and Tien, first expressing x_p as

$$x_p = x - y_o \qquad (5\text{-}6)$$

where x is the distance from the flame cylinder axis to the point where $q = q_p$. The value of x is obtained by solving the cubic equation

$$\pi y_o x^3 + (0.5h_f^2 - \pi y_o^2)x^2 = u_o^2 h_f^2 (e_b/q_p - 0.5) \ . \qquad (5\text{-}7)$$

Of the three roots of (5-7), the largest real root is always the physically correct value. The computer code is designed to select this value in all cases.

The flame height, h_f, is an important parameter in all of the expressions above. In DACFIR3 the flame height calculation method of Fang (Reference 15) is adopted with a slight modification. Fang's analysis of freely burning fires has shown that the visible flame height correlates resonably well with the point on the plume axis where the temperature of the combustion products has fallen to about 400°C (752°F) or about 2.25 times the room temperature. His relationship for the flame height is

$$h_f = (1.49 + 0.916\ K_a^{1/5})P_a^{1/5}N_b^{2/5}y_o \qquad (5\text{-}8)$$

where

$$K_a = (E_c/E_p)^4(1 - \omega)[2.25f_1 + \omega(\rho_o'T_o' - 1)/\rho_o']^3/[1.95\omega^3 f_2^3(1 - \rho_s')],$$

$$P_a = \omega f_2^2/[E_p^4(1 - \omega)],$$

$$N_b = \rho_o u_o/(\rho\sqrt{gy_o}),$$

$$f_1 = \omega(1 - \rho_o')/\rho_o' + \gamma/\chi_{o_2}^i,$$

$$f_2 = \omega/\rho_o' + \gamma/\chi_{o_2}^i,$$

$\rho_o' = \rho_o/\rho$, $T_o' = T_o/T^i$, and $\rho_s' = \rho_s/\rho$.

It can be seen that this formidable expression involves porperties of the fuel: ρ_o, u_o, γ, ω, T_o; of the exterior (to the fire) gas, χ_{o2}^i, T^i, ρ; and of the base area, y_o. In addition, the empirical entrainment constants E_c and E_p appear. Comparing (5-8) to experiments on small scale fires of n-heptane Fang found good agreement using $E_c = 0.25$ and $E_p = 0.05$. When compared to the

data on plastic fires of Modak and Croce (Reference 22), we found that the values of 0.3 for E_c and 0.25 for E_p produced better predictions of the observed flames. We have thereofre adopted these larger values for the estimation of flame lengths in DACFIR3. When entrainment is calculated for the mass conservation equations of the cabin atmosphere model the smaller values for E_c and E_p given in Section 4.3 are retained.

5.2 GAS ZONE RADIATION

In principle, a material element receives incoming thermal radiation from both gas zones and all other material elements that can be viewed from the surface of the element. However, conditions during the early stages of a cabin fire are such that only the radiation from the hot upper zone is significant. DACFIR3 includes two calculations of the radiation flux to material elements from the upper zone gas: radiation to elements which are in direct contact with the upper zone, and radiation which travels through the lower zone before reaching elements in contact with the lower zone gas. Both of these radiation fluxes are added to the flux levels described in the previous section to determine the material's fire behavior.

The computation for materials in the upper zone uses the same gray gas and mean beam length approximations as described in Section 4.5.2. The energy arriving per unit area per unit time is

$$q_{zu} = [1 - \exp(-k_u L_u)]\sigma T_u^4 \qquad (5\text{-}9)$$

where k_u is the upper zone absorption coefficient and L_u is the mean beam length. Since the element surface is in contact with the zone gas the view factor is unity.

For lower zone elements the radiation intensity from the upper zone may be reduced by absorption in the lower zone and by the view factor between the element and the lower surface of the upper zone, i.e., the thermal discontinuity plane. The flux is written

$$q_{z\ell} = \exp(-k_\ell L_\ell)F[1 - \exp(-k_u L_u)]\sigma T_u^4 \qquad (5\text{-}10)$$

where k_ℓ and L_ℓ are the absorption coefficient and beam length for the lower zone. The value of the view factor F depends on the position of the thermal discontinuity and the location of the element. To compute a separate value of F for each lower zone element is impractical for the number of elements involved so a representative view factor is used. This value is that for an element facing upward at the center of the cabin floor,

$$F = (2/\pi)[(a/A)\tan^{-1}(b/A) + (b/B)\tan^{-1}(a/B)] \qquad (5\text{-}11)$$

where $a = C_W/(z_d)$, $A = (1 + a^2)^{1/2}$, $b = C_L/(2z_d)$, $B = (1 + b^2)^{1/2}$, C_W is the compartment width at the floor, C_L is the compartment length, and z_d is the thermal discontinuity height.

SECTION 6

SAMPLE RESULTS OF THE SIMULATION OF SEVERAL CABIN FIRE TESTS

This section presents selected results from the simulation by DACFIR3 of three full-scale fire tests. These results are presented to demonstrate the cpability of the model to reproduce test results, given the best available input data. We have selected two of the most important output quantitites of DACFIR3, the predictions of gas temperature and species concentration, to compare to the experimental results. Many other quantities are included in the model's output, a complete list of which is given in Volume II.

The cabin fire tests discussed here are selected from a large series of tests conducted by Bricker, et al. (Reference 23) in a B-737 fuselage specially prepared and instrumented for repeated full scale testing. The cabin cross section measured approximately 11 feet wide at the floor and seven feet from floor to ceiling at the highest point. Moveable bulkheads (partitions) allowed for testing at two cabin lengths: 56 feet fore-to-aft giving a total cabin volume of about 3700 cubic feet; and 20 feet in length with a total volume of 1320 cubic feet. The interior lining of the cabin was lined with steel and aluminum sheet backed by high temperature resistant insulation. The lining configuration simulated a modern standard-body cabin using overhead pull-down stow bins.

Instrumentation consisted of an array of thermocouple trees for measuring air temperature, several gas sampling ports and automatic gas analysis equipment, smoke meters, flowmeters, heat flux gages, and load cells for measuring rate of weight loss during burning. Ventilation of the cabin occurred through doors in the fore and aft bulkheads. For most tests a large blower supplied a constant, known air flow directed into the cabin through the forward bulkhead door, in order to simulate a wind from an open door. Several tests were conducted without forced ventilation, the bulkhead doors being open to the exterior. This condition is termed natural ventilation.

The three tests simulated by DACFIR3 are summarized below.

Test 3B. In this test a pan of aircraft turbine fuel (Jet A) was burned in the bare (unfurnished) cabin of the 56 ft length. The objective of this test was to study the behavior of pan fires of fuel which were used as ignition sources in later tests involving materials. Located at floor level in the center of the cabin, the square pan, four square feet in area, held 4.5 liters of fuel. A load cell measured the weight loss rate of the pan during the burning period, which lasted about 10 minutes. Natural ventilation was used in this test. The dimensions of the bulkhead doors were five feet high by two and one half feet in width. The tops of the doors were five feet nine inches above the floor, leaving small sills nine inches high at the floor. Seven thermocouple trees spaced at roughly equal intervals fore-to-aft measured air temperature continuously at 20, 40, 60, and 75 inches above the floor. Measurements of gas composition were made at several horizontal positions 30 and 60 inches above the floor at 45 second intervals.

Test 5A. Conditions in this test were identical to those in Test 3B with two exceptions. First, the cabin length was 20 feet instead of 56 feet. Second, forced ventilation was employed. An airflow of 500 cubic feet per

minute (cfm) entered through the forward bulkhead door, the aft door being open to the outside. Because of the shorter length of the cabin, only five equally spaced thermocouple trees were used for air temperature. The vertical positions of the thermocouples and gas sampling ports were the same as in 3B.

Test 14A. This test, conducted using the 56-foot long cabin, involved a seat row and ceiling, sidewall, and passenger service unit (PSU) materials. A one-square foot pan of Jet A fuel burned beneath the outboard seat of a row of three surplus aircraft seats. Seat construction was of a typical wool-nylon blend fabric covering fire-retarded polyurethane foam padding. On the wall next to the outboard seat a panel of Tedlar/epoxy-fiberglass/Nomex honeycomb sidewall material extended from the floor to the PSU surface. The PSU surface was simulated by a sheet of polycarbonate stock. Both the sidewall panel and the PSU sheet were four feet in length (fore-aft direction). Ceiling panel material of the same construction as the sidewall covered a four foot length on the stow bin face surface and a 20 foot length on the ceiling proper. The bulkhead doors had the same dimensions as in Tests 3B and 5A. The ventilation was 500 cfm through the forward door.

For simulation of these tests by DACFIR, input data was collected from a number of sources. Some of these quantities, such as the cabin dimensions, ventilation, and materials location, were taken directly from the test description. One quantity, the mass burning rate of the ignition (fuel pan) fire, was obtained from the measured weight loss rates of the pan in each test. The materials flammability data for Test 14A was selected from the data set collected for the DACFIR2 validation program. This data set is described in (Reference 2). Although flammability data was not obtained from materials identical to those used in the tests, the data was obtained from materials that were nominally the same, in terms of chemical composition and physical construction. We believe that the materials data used is sufficiently characteristic of the materials used in the full-scale tests to make the comparison meaningful. Finally, a number of input quantities, such as the heat of combustion of the ignition source fuel and the thermal properties of the materials, were taken from the general literature or given "best estimate" values. In some cases the accuracy of these estimates is very good. In other cases, however, there is considerable question as to the appropriate values. When judging the performance of the model in comparison to test results, one must keep in mind the problem of providing the best estimates of the necessary input data.

Figure 11 shows the comparison of the predicted and measured gas temperature for Test 3B. The experimental curve was obtained by a simple average of the readings of the seven thermocouples at 60 inches and the seven at 75 inches. Thermocouple readings were digitized at one second intervals although only the values at each 30 seconds have been plotted in the figure. The predicted curve is the upper zone temperature from DACFIR3 computed using the measured mass loss rate of the fuel pan in the test. This rate was a very constant 0.00311 lbm/ft^2-sec throughout the first six minutes of the burn. The rate was converted to a rate of heat release by assuming an effective heat of combustion for Jet A fuel of 16,650 Btu/lbm. The effects of combustion inefficiency and sensible heat loss by flame radiation are taken into account through this effective value.

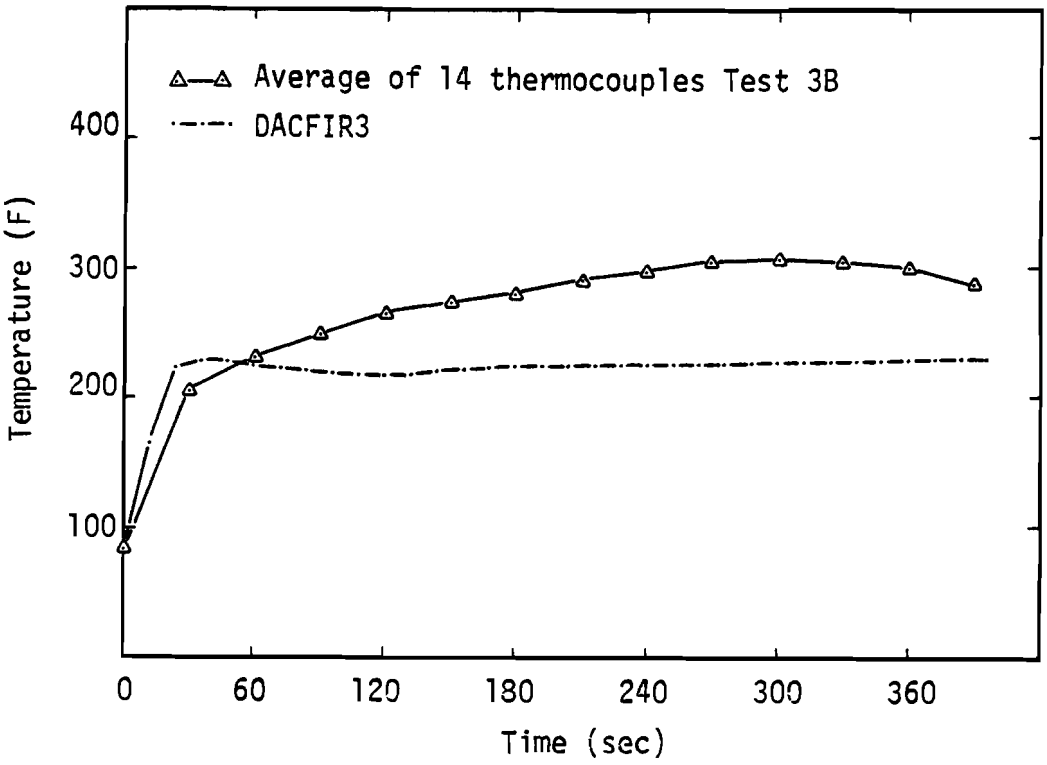

Figure 11. Predicted and Measured Upper Zone Gas Temperature for Test 3B.

The figure shows fair agreement between the prediction and the test, the maximum difference being about 80°F at 300 seconds. The intitial rate of rise of the DACFIR curve is partially determined by a feature of the model which allows the user to "ramp-in" the effect of the ignition fire over a specified period. During this period, the rates of heat, smoke, and gas release are increased linearly from zero to the constant, maximum values given in the input. From observation of the test films, a ramp-in time of 20 seconds was selected for all simulations.

After the ramp-in period, the figure shows the predicted temperature dropping slightly during the first two minutes and then rising slowly thereafter. This behavior reflects the influence of the slow heating of the walls and the subsequent decrease of heat loss from the upper zone.

The upper zone thickness computed by DACFIR for this test was quickly established at about 2.5 feet after the ramp-in period. It remained close to this value throughout the simulation. (This value of the zone thickness was used to select which test thermocouples would be averaged for the comparison.)

Another comparison of predicted and measured temperature of the accumulating hot gases is shown in Figure 12. Test 5A differed from 3B in that the cabin volume was only about one third of that in 3B and that a fixed 500 cfm forced ventialtion was used. The effect of the smaller vaolume is readily apparent in the figure where both the predicted and measured values reach about 500°F. In contrast to 3B, the prediction of temperature in 5A is higher than that measured. Again a measured burning rate from the test, 0.0058 lbm/ft^2-sec, was used as input to the simulation.

Figure 13 gives the predicted and measured gas temperature in Test 14A, the test involving materials. Figures 14 and 15 show the comparison of the

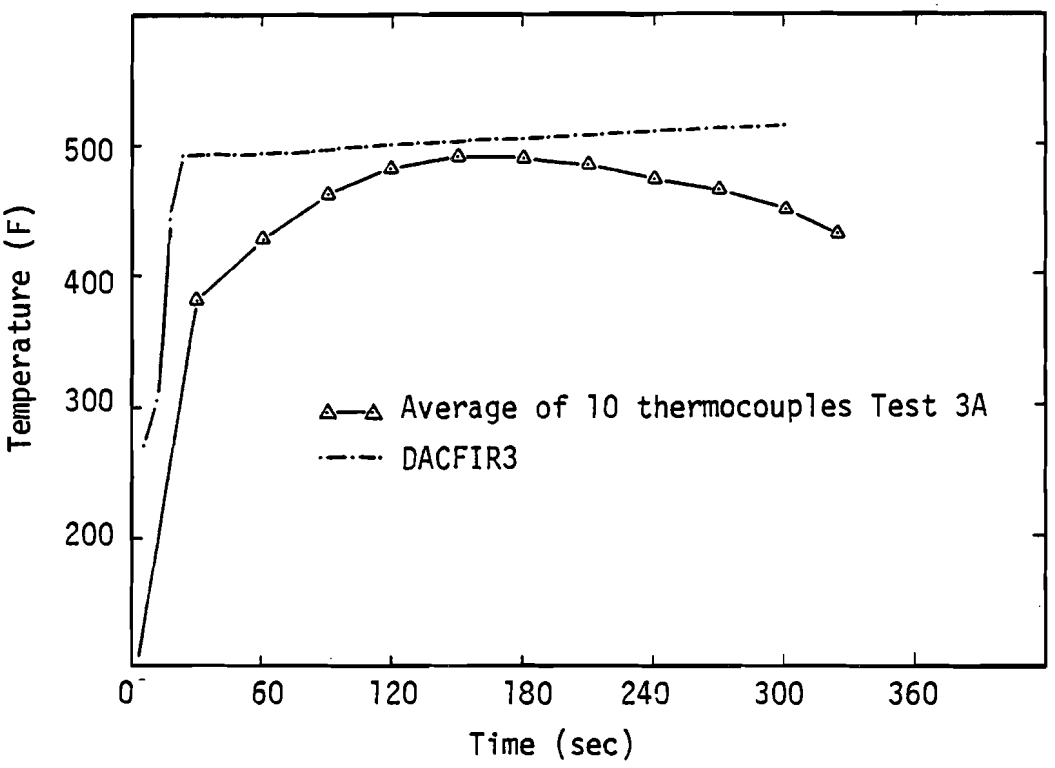

Figure 12. Predicted and Measured Upper Zone Gas Temperature for Test 5A.

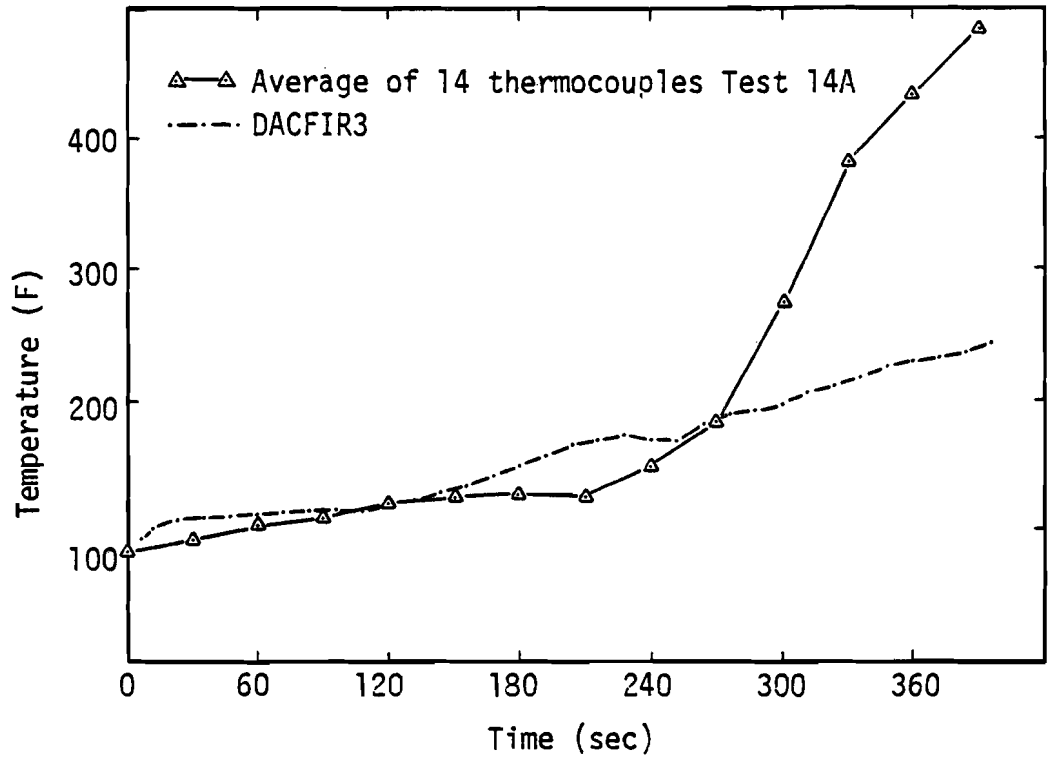

Figure 13. Predicted and Measured Upper Zone Gas Temperature for Test 14A.

predictions and measurements of three toxic gases, CO, HF and HCN. All three figures show fair agreement between prediction and measurement for the first four or five minutes. During this time the primary heat source is the ignition source fire burning at 0.00259 lbm/ft^2-sec. The pan size in this test was one square foot. As burning develops on the seat and sidewall the emissions of the toxic trace gases increase.

The model's prediction of CO accumulation is primarily ahead of the measurement while the predictions of HF and HCN are mostly behind. The noticeable recession in the predicted gas concentrations starting around four miunutes and lasting for about 30 seconds is the result of decrease in the total emission rates during this period. This decrease seems to be a consequence of the way in which the model selects fire base areas and thus flame volumes, flame radiation levels, and subsequently, emission rates.

The situation then reverses after five minutes when the predicted gas concentrations for CO and HCN begin to exceed the measurement and the HF prediction rises rapidly, closing in on the measured value at six minutes. For temperature, however, the model's prediction is well below the measurement after five minutes. The origin of the rapid temperature rise in the test results is most probably an acceleration of the burning of the seats. The seat fire in the DACFIR simulation is also growing steadily during this time but apparently not at the same rate as in the test.

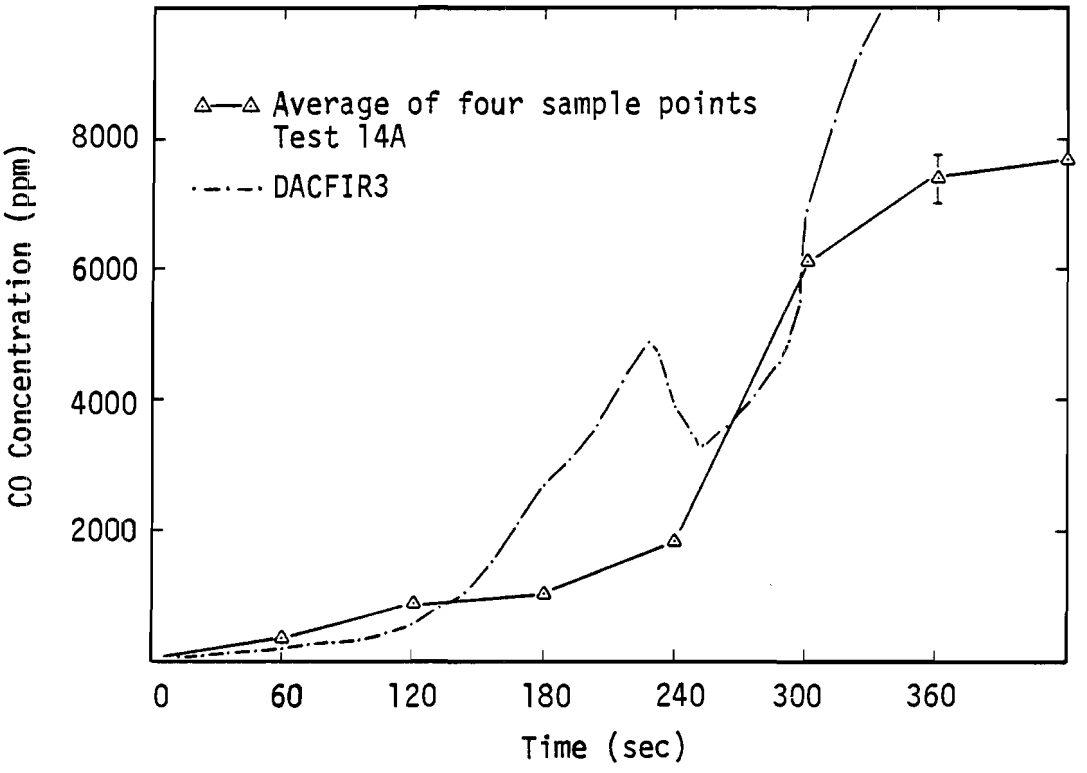

Figure 14. Predicted and Measured Upper Zone Carbon Monoxide Concentration for Test 14A.

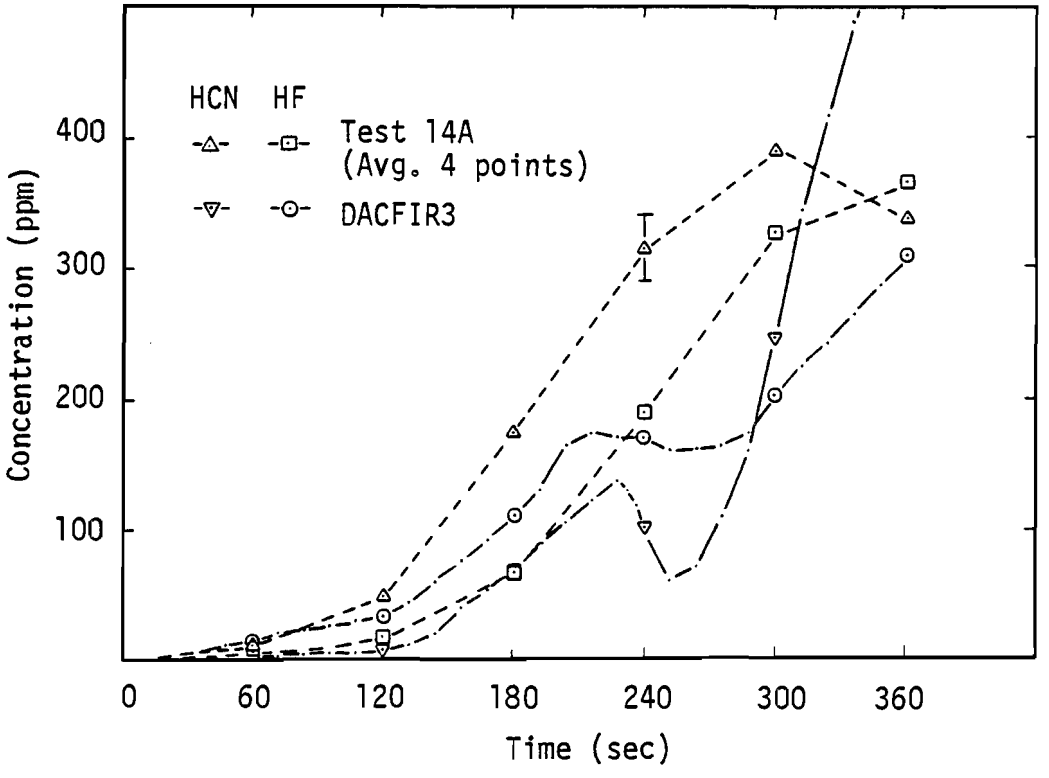

Figure 15. Predicted and Measured Upper Zone Hydrogen Cyanide and Hydrogen Fluoride Concentrations for Test 14A.

SECTION 7
CONCLUSIONS

Version 3 of DACFIR has been created as a refinement and generalization of the cabin fire model. The major differences between this version and the earlier versions of DACFIR are the revised cabin atmosphere model which allows for multiple compartments and the prescribed entry of exterior fire gases and the implicit Newton-Raphson integration technique for solution of the cabin atmosphere equation set. Major revisions have been made to the computer code to provide a more modular structure making the code easier to understand, maintain, and upgrade.

Our experience in using DACFIR3 for the simulation of three full-scale cabin fire tests has lead to the following conclusions:

(1) The implicit numerical technique for solution of the cabin atmosphere equations has proven to be superior to earlier methods in terms of both stability and computer time required. Some initial trial and error experimentation is required to find the optimum combination of integration time step, convergence tolerance, and maximum number of iterations for each case. Once this combination is identified the model appears to operate with reasonable efficiency and accuracy.

(2) The cabin atmosphere model performs adequately in predicting the average upper zone temperature for fires of constant rate of heat release. Predictions of CO_2, not shown in this report, are consistently lower than measured in the test. This problem is probably due to the oversimplified combustion chemistry assumed by the model which reflects the current lack of understanding of the fundamental behavior of turbulent, diffusion-controlled burning of liquids. Smoke and trace gas accumulation for the fuel pan fire were not compared to test results.

(3) When cabin furnishing materials were included in the fire, the model performed adequately in predicting the early development of the fire, both for temperature and trace gas accumulation. As the fire growth accelerates, the model's predictions generally lag the test results. The apparent explanation for this disagreement concerns the range of heat flux levels covered by the materials flammability data. This data, which includes ignition delay times, flame spread rates, and rates of heat and gas emission, was measured in the laboratory at imposed heat flux levels of up to about 4.5 Btu/ft^2-sec. DACFIR3's computation of the flux levels at a flame base, however, can, and often are, much higher than this value--sometimes reaching 12 or 13 Btu/ft^2-sec. To find emission rates at these high flux levels, the model linearly extrapolates from the known rates. It is quite likely that the true rates of emission, etc. at these high fluxes are not equal to the linearly extrapolated values. In particular, we might expect the high flux rates of heat release to be greater than the extrapolated values while some gas emission rates, such as CO, might be less. Relatively higher heat release rates and lower gas emission rates would result in higher upper zone temperatures and lower trace gas concentrations. It is just this situation that was observed in Test 14A.

No data was available for cabin materials at flux levels above 4.5 Btu/ft^2-sec. The current state of knowledge of solids combustion does not

suggest a trustworthy way of estimating the required information. Therefore no attempt was made to improve the extrapolation procedure. Clearly, more work, both theoretical and experimental, needs to be conducted on this problem.

REFERENCES

1. Reeves, J.B. and C. D. MacArthur, "Dayton Aircraft Cabin Fire Model," volumes I, II, and III, FAA-RD-76-120, June 1976.

2. MacArthur, C. D. and J. F. Myers, "Dayton Aircraft Cabin Fire Model Validation - Phase 1," FAA-RD-78-57, March 1978.

3. Sarkos, C. P., "Preliminary Wide Body (C-133) Cabin Hazard Measurements During a Postcrash Fuel Fire," NAFEC Tech. Letter Report, NA-78-28-LR, April 1978.

4. Eklund, T. I., "Pool Fire Radiation through a Door in a Simulated Aircraft Fuselage, "FAA Report FAA-RD-78-135, December 1978.

5. Brown, L. J., "Cabin Fire Hazards from a Large External Fuel Fire Adjacent to an Aircraft Fuselage," FAA Report FAA-RD-79-65, August 1979.

6. Eklund, T. I., "Preliminary Evaluation of the Effects of Wind and Door Openings on Hazard Development within a Model Fuselage from an External Pool Fire," NAFEC Tech. Letter Report, NA-79-1-LR, February 1979.

7. Hill, R., P. N. Boris, and G. R. Johnson, "Aircraft Compartmentation Concepts for Improving Postcrash Fire Safety," FAA Report FAA-RD-76-131, October 1976.

8. Emmons, H. W., "The Prediction of Fires in Buildings," Seventeenth Symposium (International) on Combustion, The Combustion Institute, 1978, pp. 1101-1111.

9. Quintiere, J. G., "An Approach to Modeling Wall Fire Spread in a Room," Submitted to Fire Safety Journal.

10. deRis, J., "Fire Radiation - A Review, "Factory Mutual Research Technical Report RC78-BT-27, December 1978.

11. Emmons, H. W., "Scientific Progress on Fire," Annual Review of Fluid Dynamics, Vol. 13, pp. 223-36, (1981).

12. Smith, E. E., "Measuring the Rate of Heat, Smoke, and Toxic Gas Release," Fire Technology, Vol. 8, No. 3, (1972) pp. 237-245.

13. Quintiere, J. G., "An Approach to Modeling Wall Fire Spread in a Room," Presented at the Advances in Fire Physics Conference, National Bureau of Standards, Gaithersburg, Maryland, April 1980.

14. Steward, F.R., "Prediction of the Height of Turbulent Diffusion Buoyant Flames," Combustion Science and Technology, Vol. 2, (1970), pp. 203-212.

15. Fang, J. B., "Analysis of the Behavior of a Freely Burning Fire," NBSIR 73-115, Feb. 1973, U.S. National Bureau of Standards, Washington, D.C.

16. Tanaka, T. "A Model on Fire Spread in a Small Scale Building," in M. A. Sherald, Ed. Fire Research and Safety, Special Publication 540, National Bureau of Standards, Nov. 1979.

17. Emmons, H. W., C. D. MacArthur, and R. Pape "The Status of Fire Modeling in the United States - 1978," Presented at the 4th Joint Meeting, U.S. - Japan Panel on Fire Research & Safety, UJNR, Tokyo, Japan, 1979.

18. Quintiere, J. G., "The Growth of Fire in Building Compartments," in A.F. Robertson, Ed., Fire Standards and Safety, Special Publication STP 614, American Society for Testing and Materials, 1977.

19. Emmons, H.W., H. E. Mitler, and L. E. Trefethen, "Computer Fire Code III," Home Fire Project Tech. Report 25, Harvard University, Jan. 1978.

20. Dayan, A. and Tien, C. L., "Radiant Heating from a Cylindrical Fire Column," Combustion Science and Technology, Vol. 9, 1974, pp. 41-47.

21. Fu, T. T., "Aviation Fuel Fire Behavior Study," U.S. Naval Civil Engineering Laboratory, AGFSRS 72-2, February 1972.

22. Modak, A. T., and Croce, P. A., "Infludence of Flame Radiation on the Burning Rate of Plastic Pool Fires of Varying Scale," Paper Presented at the Ninth Fall Technical Meeting 1975, Eastern Section: The Combustion Institute, Nov. 6-7, 1975, SONY at Stony Brook, Long Island, New York.

23. Bricker, R. W.,et al., Report in preparation, NASA Johnson Space Center, Houston, Texas.

☆U.S. GOVERNMENT PRINTING OFFICE: 1982 505 067 13